BSGF - Earth Sciences Bulletin 2021, 192, 53
© N. Blond *et al.*, Published by EDP Sciences 2021
https://doi.org/10.1051/bsgf/2021041

BSGF Earth Sciences Bulletin

Available online at:
www.bsgf.fr

Special Issue Gearcheology J. Curie, S. Vandevelde, A. Quiquerez and C. Petit (Guest editors)

Open Access

From section to landscape(s): reconstructions of environmental and landscape changes for the past 8000 years around the site of Wakarida (Ethiopia) using chronostratigraphy

Ninon Blond[1,2,*], Nicolas Jacob-Rousseau[1], Charlène Bouchaud[3] and Yann Callot[1]

[1] UMR 5133 Archéorient, Université Lumière Lyon 2, 5 Avenue Pierre Mendès, 69676 Bron, France
[2] UMR 5600 EVS, ENS de Lyon, 15 Parvis René Descartes, 69342 Lyon, France
[3] UMR 7209 Archéozoologie, Archéobotanique, Sociétés, Pratiques, Environnements, CNRS/MNHN, 55 rue Buffon CP56, 75005 Paris, France

Received: 17 November 2019 / Accepted: 24 September 2021 / Publishing online: 3 November 2021

Abstract – In northern Tigray (Ethiopia), the combined presence in the valley bottoms of sedimentary fills several meters thick and of archaeological remains of human settlements (homes, camps) raises the question of the socio-environmental processes at the origin of these deposits and their interactions with human populations. However, in certain (national, legislative) contexts, it can be difficult to apply very advanced techniques or to perform a large number of analyses. This paper shows that a chronostratigraphic approach based on laser granulometry, loss on ignition and radiocarbon dating provides satisfactory answers to the main geoarchaeological questions. Our specific objective was to reconstruct the landscape and environmental changes in the region around the Wakarida archaeological site, based on the sedimentary deposits in the valley bottoms. These deposits are now cultivated by the inhabitants, thanks to the construction of agricultural terraces in the 20th century. Archaeological excavations unearthed an urban settlement at Wakarida which dates from the classical Aksumite (150–400/450 AD) and post-Aksumite (800/850 AD) periods, and traces of earlier archaeological occupations (pre- and proto-Aksumite periods, 800–50 BC) in the study area. These remains raise questions about the influence of societies on their environment. A method based on a combination of fieldwork, sedimentological analyses and dating was used to answer these questions. This chronostratigraphic study is partially based on the identification of chronological inversions, revealing ablation and depositional phases in the sedimentary cascades, which have to be taken into account to understand the evolution of the site. We identified several phases in the establishment of the present-day landscape around the Wakarida site. During the Northgrippian (Early Holocene), the valleys were progressively filled by low-energy alluvial and/or colluvial processes. During the Meghalayan (Middle Holocene), ablation processes alternated with depositions resulting from climatic processes and possible anthropogenic influences. From the 1st millennium BC, the impact of the population on its environment (deforestation) has resulted in chronological inversions in the deposits, particularly around the 14th and 17th centuries AD.

Keywords: chronostratigraphy / chronological inversion / geoarchaeology / landscape / Ethiopia / Wakarida

Résumé – De la coupe au(x) paysage(s) : reconstitutions des changements environnementaux et paysagers depuis 8000 ans autour du site de Wakarida (Éthiopie) grâce à la chronostratigraphie. Dans le Nord du Tigray (Éthiopie), la présence conjointe de remplissages sédimentaires de plusieurs mètres d'épaisseur dans les fonds de vallées et de vestiges archéologiques d'implantations humaines (habitat, campements) pose la question des processus socio-environnementaux à l'origine de ces dépôts et de leurs interactions avec les populations humaines. Cependant, dans certains contextes (nationaux, législatifs), il peut être difficile d'appliquer des techniques très avancées ou d'effectuer un grand nombre d'analyses. Cet article vise à montrer qu'une approche chronostratigraphique s'appuyant sur de la granulométrie laser, des analyses par perte au feu et des datations radiocarbones, apporte des réponses satisfaisantes aux principales questions géoarchéologiques. L'objectif est ici de reconstruire les changements paysagers et

*Corresponding author : ninon.blond@ens-lyon.fr

environnementaux de la région autour du site archéologique de Wakarida, en s'appuyant sur les dépôts sédimentaires de fonds de vallées. Ces dépôts sont aujourd'hui cultivés par les habitants grâce à la construction de terrasses agricoles, établies au XX^{e} siècle. Les fouilles archéologiques ont mis au jour un peuplement urbain à Wakarida, datant des périodes axoumite classique (150–400/450 ap. J.-C.) et post-axoumite (800/850 ap. J.-C.), et des traces d'occupations archéologiques plus anciennes (périodes pré et proto-axoumites, 800–50 av. J.-C.) dans la zone d'étude. Ces vestiges interrogent le rôle joué par les sociétés sur leur environnement. Pour répondre à ces questions, une méthode basée sur une combinaison de travaux de terrain, d'analyses sédimentologiques et de datations a été utilisée. Cette étude chronostratigraphique repose en partie sur la mise en évidence d'inversions chronologiques, révélant des phases d'ablation et de dépôts dans les cascades sédimentaires, dont la prise en compte est nécessaire à la compréhension de l'évolution du site. Nous avons ainsi identifié plusieurs phases dans l'établissement des paysages actuels autour du site de Wakarida. Au cours du Northgrippien (Holocène ancien), les vallées ont été progressivement comblées par des processus alluviaux et/ou colluviaux de faible énergie. Pendant le Méghalayen (Holocène moyen), les processus d'ablation alternent avec les dépôts, conséquence des processus climatiques et d'éventuels processus d'origine anthropique. À partir du I^{er} millénaire av. J.-C., l'impact de la population sur son environnement (déboisement) se traduit par des inversions chronologiques dans les dépôts, particulièrement autour des XIV^{e} et XVII^{e} siècles ap. J.-C.

Mots clés : chronostratigraphie / inversion chronologique / géoarchéologie / paysage / Éthiopie / Wakarida

1 Introduction

Geoarchaeology makes it possible to understand the relationships between societies and their environment on a long timescale. However, it is not always possible to perform a large number of advanced analyses (for example, in geochemistry). This paper shows that basic chronostratigraphic studies (sedimentological, stratigraphic, and chronological analyses) can provide robust answers to the main geoarchaeological questions.

The geoarchaeology of Tigray is a quite recent field of study. The starting point for these studies was Butzer (1981)'s article. He argues that the fall of the Aksumite Kingdom in the 8th century AD is related to the climate and the overexploitation of the environment by the inhabitants. This included forest clearing leading to the erosion of the sediments on the slope, as they were no longer protected by the vegetation (Butzer, 1981).

The objective of this article is trans-scalar: moving from the study of stratigraphic sections, uncovered in valley bottoms filled by sedimentary deposits, to the reconstruction of landscape and environmental changes in the area, in connection with the archaeological site of Wakarida (northern Tigray, Ethiopia). The study area is located on the margin of the Tigray plateau. The valleys are filled with sediment and are cultivated, while the inhabitant's homes are built on flat areas of the slopes. The climate is dry, and the current vegetation is low-growing (shrubs).

The presence of archaeological remains (human settlements in the form of stone constructions or camps, potsherds) in this densely occupied area raises questions about the interactions of populations with their environment over time. Chronostratigraphy, based on stratigraphic observation, sedimentology, and radiocarbon dating, make it possible to identify the main processes at work in the formation of the current landscapes and the changes they have undergone to identify the respective roles of biophysical and climatic processes and of human actions, and their consequences in terms of landscape (afforestation, erosion, land use).

This article is based on the field work, laboratory analyses and dating undertaken to achieve these objectives. The samples were collected during three field campaigns (2014, 2015 and 2017).

2 Geographical, archaeological and geoarchaeological context

2.1 Geographical settings

The archaeological site of Wakarida (14°16'21.00"N, 39°44'18.80"E) is located in the northernmost part of Tigray (Ethiopia), some 30 km as the crow flies south of the border with Eritrea (Fig. 1). In this area, the topography gradually rises from west to east, from Sudan to Ethiopia then drops sharply before the Afar depression. The study area (50 km^2) belongs to the topographic unit called "Northern Highlands" (Billi, 2015) and is situated on the margins of the Tigray plateau, at an altitude of between 2300 and 2500 m asl (Fig. 1). It consists of steeply sloping valleys.

The Wakarida area and its surroundings are located on sedimentary and/or metamorphic deposits. The study area comprises two main groups, both Precambrian, and a third group which covers only a small portion of the territory (Fig. 2). The first group is represented by the Tsaliet Group, which consists of "intermediate and basic lavas, greywacke, tuffaceous slate, phyllite, agglomerate and rhyolite" and corresponds to the eastern part of the surveyed area (Kazmin, 1976). The other set is the Didikama Formation, which is composed of "dolomite interbedded with slate". Finally, the Arequa Formation, which includes "undifferentiated slates, phyllites, calcareous sediments and limestones" (Kazmin, 1976) is situated at the far east of the area. The partition between the two major units follows the path of a NNE-SSW fault (Kazmin, 1976). Overall, the fault lines guide the implementation of the hydrographic network (Fig. 2).

Today, the valleys are filled with sediments, and no permanent flow crosses their floor. Apart from exceptional flood periods, all flows are underground. The hydrology is

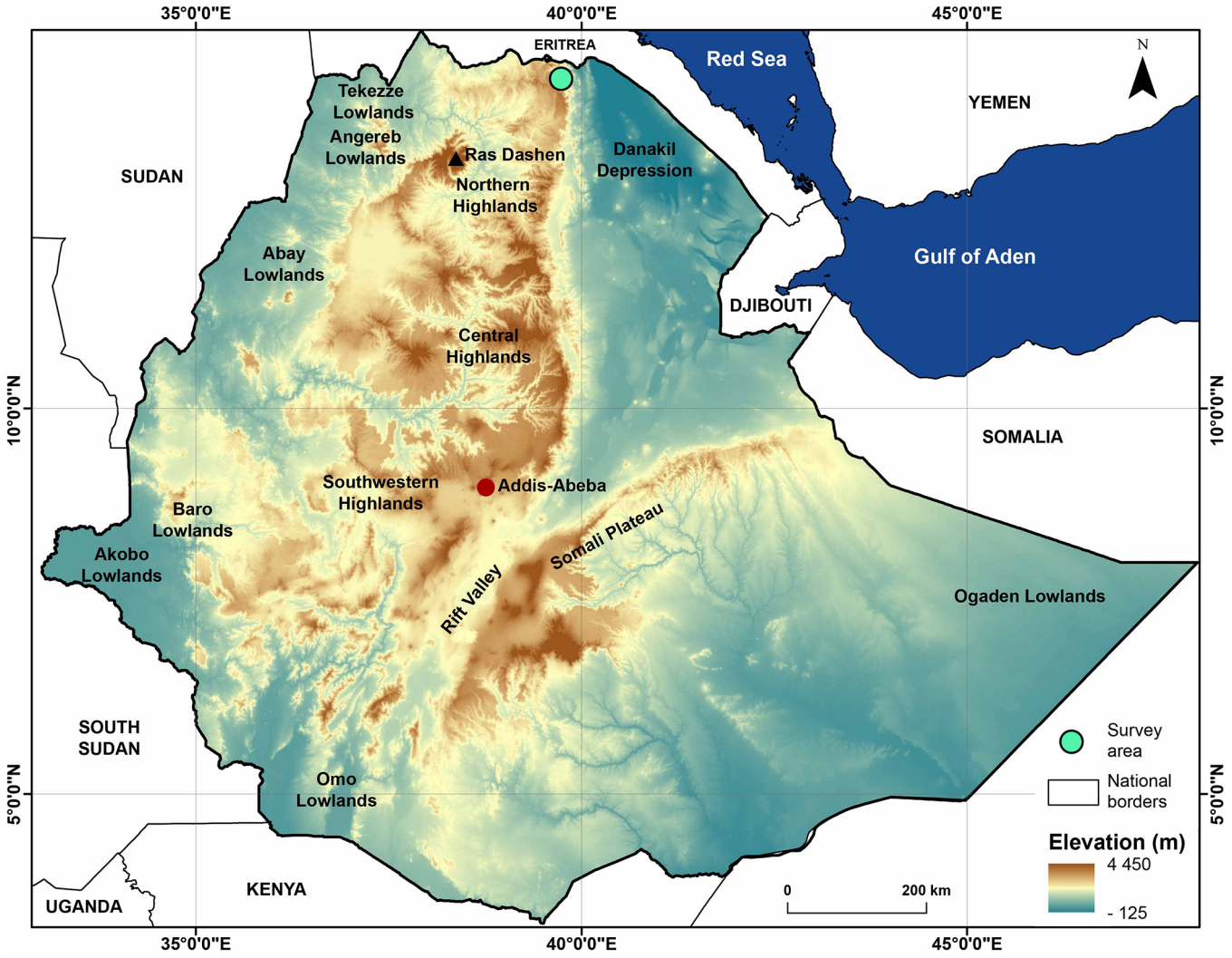

Fig. 1. Topographical units of Ethiopia and location of the survey area. Elevation from STRM 30 m.
Fig. 1. *Unités topographiques d'Éthiopie et localisation de l'espace étudié. Altitude d'après SRTM 30 m.*

strongly influenced by the climate of the area, especially by rainfall distribution. There are two rainy seasons and one dry season in northern Tigray (Bascom, 2015): most rain falls between June and September (*kiremt*), after a rainy season with less rainfall between February and May (*belg*). The dry season extends from October to January and is called *bega*. Mean annual rainfall in the area ranges from 379 mm/yr to 575 mm/yr, and *kiremt* rains represent between 57 and 62% of the total rainfall (Blond *et al.*, 2018).

The present-day climatic conditions were established in the 2nd mill. BC, with a short humid phase between 500 BC and 500 AD (Bard *et al.*, 2000). Before that, the climate was wetter than today, in line with the African Humid Period (AHP), which occurred between 15 000 and 5 000 BP, with variations according to latitude and longitude (Shanahan *et al.*, 2015). The concentration of rainfall has consequences for agriculture, which is mainly based on cereals (barley, maize, teff, wheat, millet, sorghum) and leguminous plants (chickpeas, faba beans, horse beans or field peas, Edwards *et al.*, 2007). The crops are grown on sediments deposited at the bottom of the valleys. These sedimentary fills are cultivated using terraces, built perpendicular to the direction of the valley, blocking the thalweg from one bank to another. Homes are located on high spots (hilltops, topographic passes). Terraces are signs of the adaptation of today's populations to a challenging environment: soil and water resources being scarce, the terrace walls are built to enhance agricultural production by concentrating water on the plots and protecting the soil from erosion (Fig. 3). Studies have shown that these terraces are of recent construction (Blond *et al.*, 2018; Blond, 2019), but the sedimentary deposits on which they rely provide records of changes in the environment and of the impacts of human activities on the landscape.

2.2 Archaeological context

The archaeological site of Wakarida was discovered in 1996 by Ato Tekle Hagos and Ato Habtamu Mekonnen during surveys organized by the Tigrai National Regional State Culture and Tourism Agency (TCTA). The locals told them that while searching for stones to build their own houses, they had uncovered quadrangular rooms. Since 2010, the site has

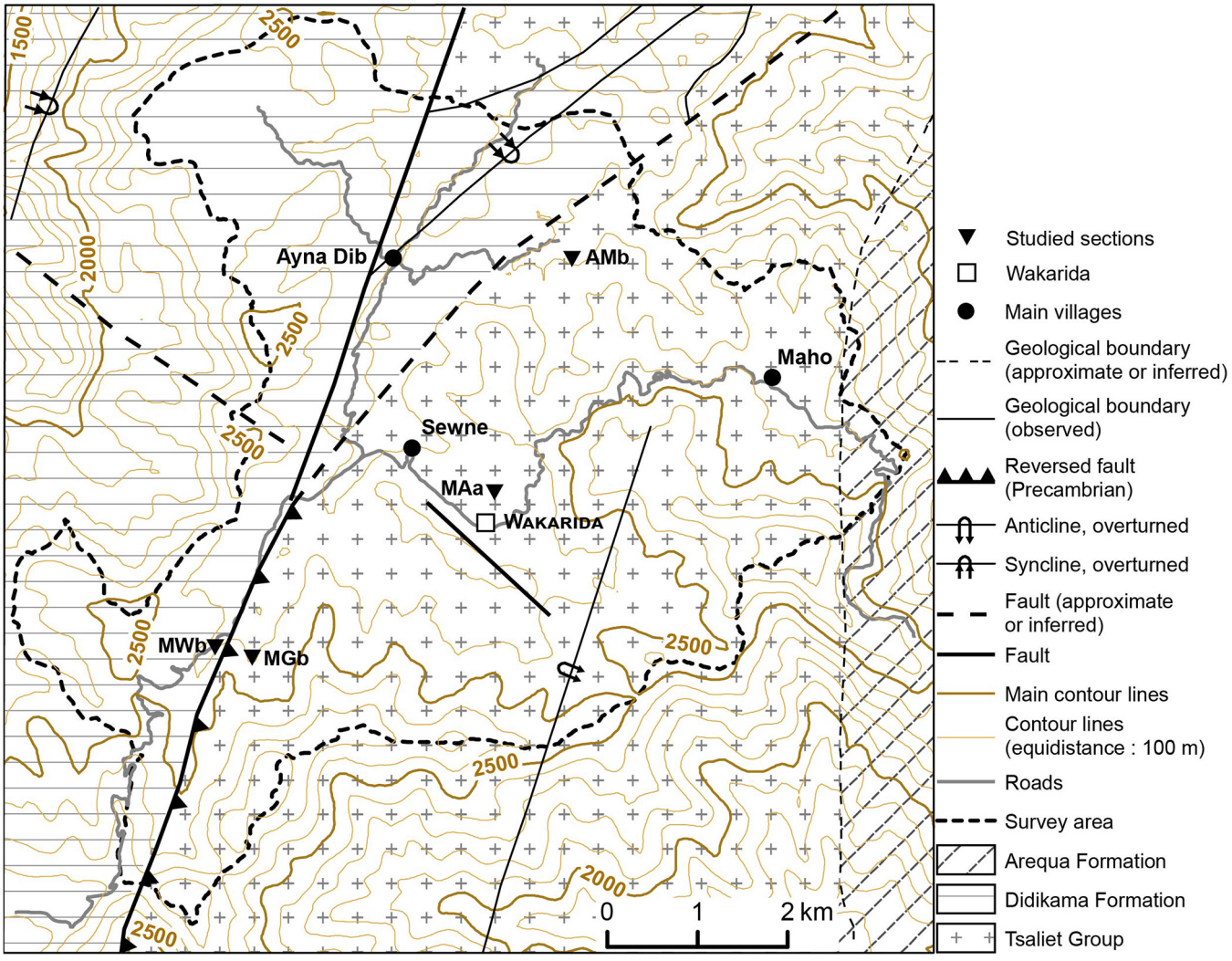

Fig. 2. Geological sketch of the study area. Geology after Kazmin (1976), MAFTOR GIS.
Fig. 2. *Croquis géologique de la zone étudiée. Géologie d'après Kazmin (1976), SIG MAFTOR.*

been excavated by the Franco-Ethiopian archaeological mission in the Eastern Tigray (MAFTOR), led by Anne Benoist and Iwona Gajda (Dugast and Gajda, 2010).

The site of Wakarida is located on a spur at the northernmost end of the Tigray Plateau and on the margins of the Aksumite kingdom (Dugast and Gajda, 2010). It consists of an Aksumite agglomeration of medium size, featuring prestigious buildings dating from the classical Aksumite (150–400/450 AD) and the post-Aksumite periods (800/850 AD) (Gajda *et al.*, 2017). The surrounding survey area contains older remains dating from the pre- and proto-Aksumite periods (800–50 BC), mainly potsherds and traces of buildings (Gajda *et al.*, 2017; Benoist *et al.*, 2020). Occupation has been dated through chrono-cultural evidence (building styles, potsherds) and radiocarbon dating (Dugast and Gajda, 2010; Gajda *et al.*, 2017; Benoist *et al.*, 2020)

The study area is marginal in relation to the centre of the Aksumite kingdom around the city of Aksum, in Central Tigray (Gajda *et al.*, 2017). In other places in the kingdom, Aksumite occupation is reflected by monumental buildings, temples, or stelae, but also smaller settlements with domestic and agricultural functions (Finneran, 2007).

The archaeological findings described above raise the question of the relations between ancient populations and their environment and their agricultural practices.

2.3 Socio-ecological systems in Tigray: a state-of-the-art approach

Evidence of the impact of population on their environment is relatively scarce in Tigray. Bard *et al.* (2000) reported that the arrival of people on the plateau led to the opening up of the vegetation through the wood felling. The vegetation was gradually cleared at the beginning of the 2nd millennium BC. Between the 2nd millennium and 800 BC, research revealed the first traces of deforestation and intensive agriculture on the slopes around Yeha (Pietsch and Machado, 2014), which resulted in strong colluviation. Gebru *et al.* (2009) attribute the

Fig. 3. Terraces in May Ayni Valley. Valley bottoms are cultivated, whereas the slopes are barren.
Fig. 3. *Terrasses dans la vallée de May Ayni. Les fonds de vallées sont cultivés, tandis que les versants sont nus.*

deforestation to the need to maintain the Aksumite kingdom. Between the 1st millennium BC and the first half of the 1st millennium AD, very high demographic pressure led to the colonisation of the entire area, even land of limited agricultural value (Berakhi *et al.*, 1998; Bard *et al.*, 2000). The depopulation of the region during the post-Aksumite period resulted in the regeneration of vegetation at the beginning of the 2nd millennium AD (from 779 to 1032 AD around Adigrat, according to Bard *et al.*, 2000).

3 Material and methods

3.1 Field work

Field work focused on the identification of sections or erosion forms and the drawing of a geomorphological map. The geomorphological survey of the area was completed by sampling of the sections. Samples were not collected regularly, but at each change of facies. The faciological criteria are grain size, sediment organisation and colour. When present, fragments of charcoal were also hand-picked, for the purpose of dating.

The survey covered the whole study area. Four sites were selected in the local catchment, distributed from upstream to downstream (Fig. 4). At the scale of the survey area, May Weini b (MWb) forms the upstream part, and Ambare b (AMb) the downstream part. MWb is located in an intermediate position in May Weini valley. Mengangebit b (MGb) is situated in the locality of Mengangebit in the upstream part of this small tributary of May Weini valley. Like MWb, May Ayni a (MAa) is in an intermediate position in May Ayni valley. AMb, located downstream of the system, also forms the downstream part of Ambare valley, and the valley turns into a gorge a short distance farther on. Unlike MWb, MAa and AMb, which are located in the main valley, MGb was chosen because it is a good example of a sub-drainage basin.

3.2 Sedimentological analyses

The studied sections were chosen as representative of the different parts of the local catchment (upstream/downstream/intermediate position, see above), but also for the time span they cover, which allows the study of a wide chronology, from 7th millennium BC (9th millennium BP) to 17th century AD (4th century BP) as seen below in the Chronostratigraphic Results section. Due to lack of time and funding, no sediment sample was taken in MGb. The section was dated, and the stratigraphic organisation described on-site.

3.2.1 Description of the sections

The MWb section is located in a narrow part of the May Weini Valley, where the slope is low, the two slopes are close and the road passes through. MWb is located downstream of a confluence with a small steep valley (Fig. 2). The cross-section is 330 cm thick, but did not reach the bedrock. The section is located on the right bank of the valley and cuts through a colluvio-alluvial deposit placed against the slope.

MAa is not a natural section but a well recently dug in the embankment of the valley by the current inhabitants. When first visited, it allowed observation of the stratigraphy to a depth of seven metres. In 2020, it had been dug deeper with an excavator, the surface of the water now reaches 820 cm (Fig. 5). This section is located in a flat topographic area in the thalweg (Fig. 6A), below the archaeological site of Wakarida (Fig. 4). At this point, the valley widens before again narrowing between the spur of Wakarida on the left bank and a slope on the right bank. The well is located approximately in the centre of the valley, slightly offset towards the right bank. The rectangular configuration of the well makes it possible to observe the longitudinal and lateral organisation of the sediments (Figs. 6A and 6B). Access to the first few metres below the surface is made possible by a staircase carved in the downstream side of the well, which allows the owner to get closer to the surface of the water and install a motor pump (Fig. 6B). As the well contained water at the time of sampling (November 2017), we were unable to see the bottom. The bottom, which was measured in 2018, was 8.4 m below the surface. The depth of water is thus estimated at 1.4 m although it was not measured in 2020. The first three metres above the surface of the water are made up of large blocks, while the top four metres alternate fine material and gravel.

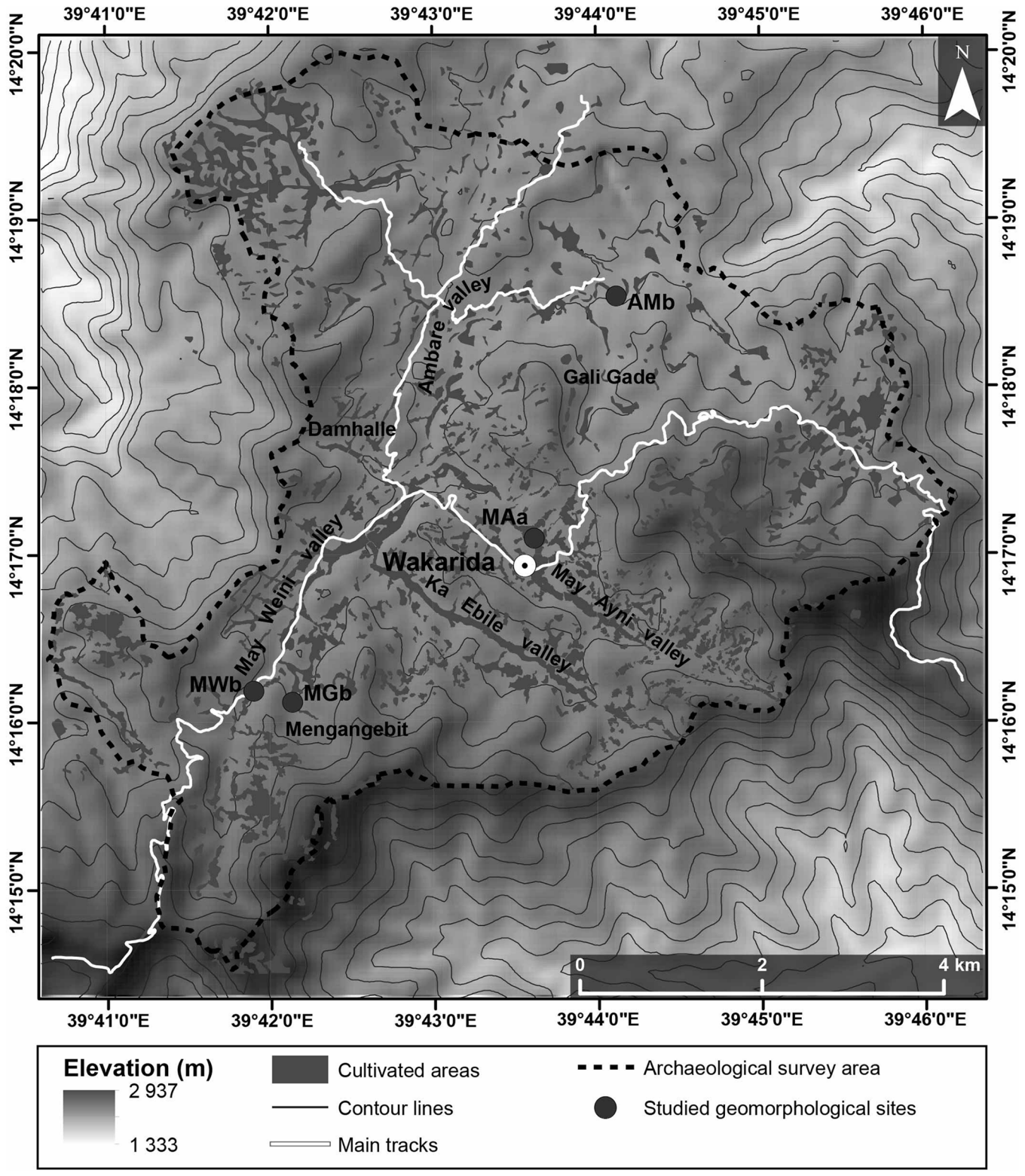

Fig. 4. Map of the geomorphological sites in the survey area. Elevation from SRTM 30 m, MAFTOR GIS.
Fig. 4. *Carte des sites géomorphologiques étudiés au sein de la zone d'étude. Altitude d'après SRTM 30 m, SIG MAFTOR.*

Fig. 5. The MAa well in May Ayni Valley (see Fig. 6) after deepening in 2020.
Fig. 5. *Le puits de MAa dans la vallée de May Ayni (*cf. *Fig. 6) après l'approfondissement de 2020.*

The Mengangebit site is located in a kind of recess at the bottom of the valley, which may explain why the sediments were protected (Fig. 4). The site is quite big: the deposit can be traced for more than 100 m. The deposit is pressed against a slope on the left bank and some flakes of the valley fill are still visible on the right bank. This colluvio-alluvial deposit is organised in a dejection cone located at the outlet of two small ravines. It appears at the level of a widening zone of the valley, which is particularly narrow upstream. When cleared of this accumulation, the erosion front runs parallel to the flow direction of the valley. It has been laid out in terraces, but the bed of the river remains visible: the entire thalweg is not blocked, and traces of the flows are still visible. The actions taken to enable cultivation are reflected in the presence of dry-stone walls. Only one area, at an intermediate level between the two levels of terraces, is not covered by the wall (Fig. 7). It is in this accessible area that it was possible to study the MGb section.

In Ambare, the section is more than ten metres long, it is located on the right bank, parallel to the flow direction. AMb is located downstream, shortly after the confluence with a thalweg draining a watershed of several dozen hectares (Fig. 4). This section was cleared by lateral erosion of colluvio-alluvial sedimentary fills in the valley bottom. The alluvial groundwater outcrops at several points, marked by small areas of stagnant water. It is a fairly narrow valley, which ends in a gorge about 900 m as the crow flies downstream of AMb (Fig. 8).

The section is located at the beginning of a meander concavity on the right bank (Fig. 8). It is linked to the erosion that has cut into the valley bottom fill, exposing the stratigraphy over a distance of several metres. Upstream of the meander, the deposit was preserved on the right bank; inside the meander, it was preserved on the left bank (Fig. 8). Its top is cultivated.

3.2.2 Sedimentological methods and indices

The sedimentological analyses were performed at the OMEAA (*Observatoire et Mesure des Environnements Actuels et Anciens*) platform in Lyon. The two main techniques used were grain size analysis and Loss on Ignition (Heiri *et al.*, 2001).

Grain sizes were measured using two different techniques. First, sieves were used to determine the granulometric texture. The sample was placed on the sieve column and sieved with water. Four sieves with following mesh sizes were used, 63 μm, 500 μm, 2 mm and 10 mm. They made it possible to determine five granulometric classes: fine particles (clay and silt, < 63 μm); fine sands (63–500 μm); coarse sands (500 μm–2 mm); fine gravels (2–10 mm) and coarse gravels (> 10 mm).

Grain size analyses were also performed on the finer < 2 mm fraction, using a laser granulometer. For this purpose, between 5 and 8 g of the sample were transferred in a beaker placed in a sand bath and heated to 80 °C. The organic matter was destroyed with 110-volume peroxide attacks. After destruction of the organic matter, the content of each beaker was transferred in a centrifuge tube with potassium chloride to remove the Ca^{2+} flocculating ions. The sample was then washed with deionized water to remove chlorine. After rinsing, sodium hexametaphosphate was added in the tube to disperse the sediment. After agitation, the sample was divided into aliquots and finally poured into the granulometer for measurement. To facilitate comparison of the different textures determined by wet sieving and grain size measured by laser granulometry, we decided to apply the same classification, using three main classes: fine fraction (clay and silt, < 63 μm); sandy fraction (63 μm–2 mm) and coarse fraction (> 2 mm).

The GRADISTAT program (Blott and Pye, 2001) also enabled the calculation of useful indices: mean, median, mode, sorting, skewness, and kurtosis. Due to the marked heterogeneity of the series and poor sorting of the sediments, we decided not to use the Trask indices (sorting and skewness), as they focus on a reduced part of the distribution, only the first, second and third quartiles (Trask, 1930), thus neglecting the extremities of the distribution. For the same reason, we decided to use the indices of Folk and Ward (1957) rather than those of

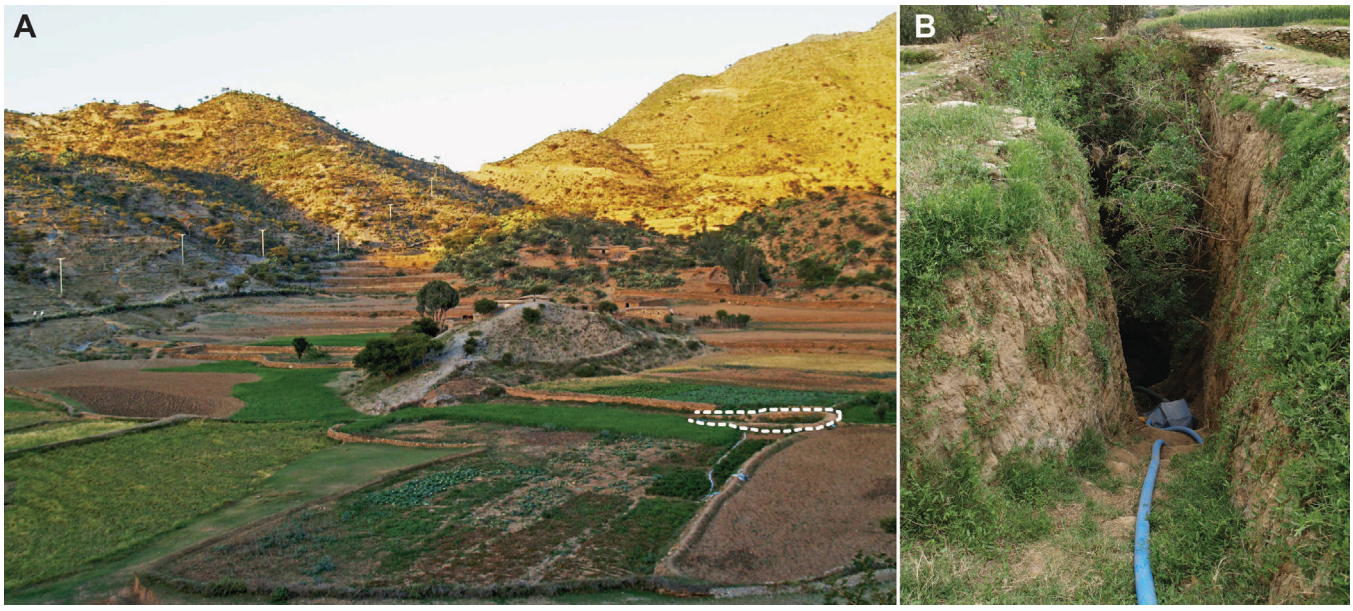

Fig. 6. A: Location of the MAa well in May Ayni Valley; B: MAa section in the well.
Fig. 6. *A : Localisation du puits MAa dans la vallée de May Ayni ; B : coupe MAa dans le puits.*

Fig. 7. Site of the Mengangebit sections.
Fig. 7. *Site des coupes de Mengangebit.*

Inman (1952). The synthetic formulae proposed by Folk and Ward (1957) were summarized and modified by Blott and Pye (2001). Thus, our analysis relies on the Folk and Ward geometric method as modified by Blott and Pye (2001) for the determination of sedimentological indices.

In addition to grain size analyses, organic matter and calcium carbonates contents were measured using the Loss on Ignition technique (LOI, Heiri *et al.*, 2001). This technique provides good insights into the physico-chemical composition of the samples. First, the samples were pre-dried in beakers overnight in an oven at a temperature of 50 °C. A 1,000 g aliquot was then taken from the beakers, crushed, and poured into crucibles that had also been oven-dried for one night. Each empty dry crucible was weighed individually on a precision balance. The combined mass of the dry crucible and sample was recorded. The samples were then placed in a Nabertherm Muffle Furnace, first for five hours at 550 °C, then a second time for two hours at 950 °C. After each oven run, the samples were cooled to room temperature, dried in the oven if necessary and weighed with a precision balance. After subtracting the mass of the crucible, the first weighing gave the mass of organic matter destroyed during the baking process. The second weighing gave the calcium carbonate mass lost. These masses were related to the starting dry sample mass to obtain the organic matter and calcium carbonate content originally present in the samples.

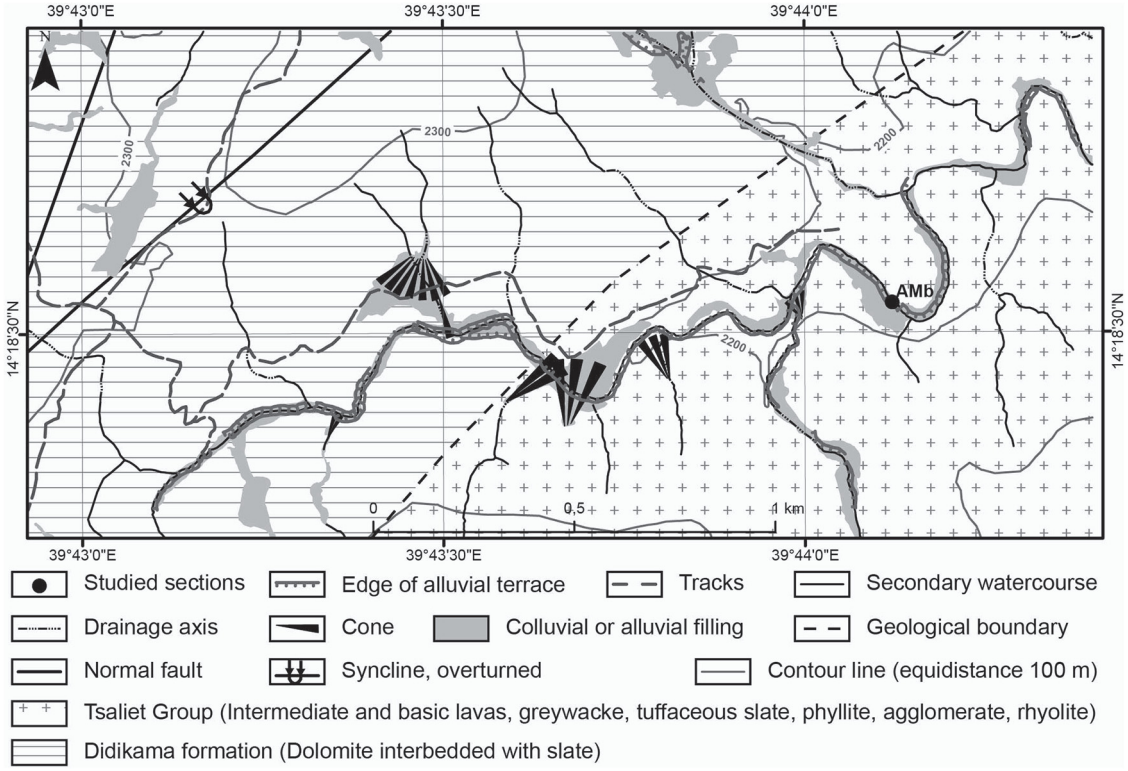

Fig. 8. Geomorphological sketch of Ambare Valley and its surroundings. Geological information after Kazmin (1976).
Fig. 8. *Carton géomorphologique de la Vallée d'Ambare et de ses alentours. Géologie d'après Kazmin (1976).*

3.3 Dating

Finally, when it was possible to find charcoal in the section, the samples were dated using radiocarbon dating. As the quantities were very low, the AMS (Accelerator Mass Spectrometer) technique was used. The samples were sent to the Saclay ARTEMIS accelerator. Due to the small quantities, charcoal fragments could not be identified prior to dating. In Table 1, ages are given in years BP (radiocarbon ages), in calibrated years BP, with two sigma precision and using the calibration curves of Reimer *et al.* (2013), and are also given in cal. BC/AD (calibrated calendar ages). In the figures and in the text, the ages are expressed in cal. BP.

3.4 Charcoal analyses

In addition to the charcoal sampled for radiocarbon dating, some charcoals were sampled for the purpose of identification. Charcoal fragments were split by hand along the three diagnostic planes (transversal, longitudinal-tangential and longitudinal-radial) and observed with an incident light microscope (Olympus BX51M) at the archaeobotanical platform of the French National Museum of Natural History (AASPE laboratory, UMR 7209).

Taxonomic determination was performed using the modern charcoal reference collection, the wood anatomy atlases (Schweingruber, 1990; Neumann *et al.*, 2001), plus the "Inside Wood" Internet database (https://insidewood.lib.ncsu.edu/search?3). All the charcoal pieces examined were identified.

4 Chronostratigraphic results and interpretations

In this section, we first present our main general observations concerning the stratigraphy and the organic matter and calcium carbonate contents of the samples. We then present the detailed results and our interpretation of the stratigraphic observations, grain size and dating analyses for each section. The two last subsections provide a synthesis of anthracological analyses and of all the radiocarbon dates. The sections are presented from upstream to downstream in the study catchment (Fig. 4). Where possible, the stratigraphy was analysed through wet sieving, laser granulometry and Loss on Ignition (LOI) analyses (AMb, MAa and MWb). In the MGb section, no sedimentological analyses were performed.

4.1 General observations

4.1.1 Grain size distribution and indices

Laser granulometry of the sediments revealed high homogeneity: almost all the sediments were mainly comprised of fine particles (silt and clay) with variable amounts of sand. Grain-size analyses showed that 38 of the 42 samples were composed of more than 50% silts. The three samples in which a coarse fraction was detected contained less than 50% silts. Thus, most of the samples analysed using laser granulometry were rather fine, with clay contents rarely exceeding 10%. These similarities also appeared in some of the statistical indices, such as the modes: the first mode of 34 out of the

Table 1. Radiocarbon ages of the four sections studied.
Tableau 1. *Âges radiocarbones des quatre coupes étudiées.*

Section	Sample code	Depth (cm)	Material	Laboratory code	Radiocarbon age	Calibrated radiocarbon age (cal. BP, 2 sigmas)	Calibrated calendar age (2 sigmas)
MGb	**MGb01ch**	110	Charcoal	Lyon-15269	3780 ± 30 BP	4245–4009	2296–2060 BC
	MGb02ch	140	Charcoal	Lyon-15270	3810 ± 30 BP	4347–4090	2398–2141 BC
	MGb04ch	155/160	Charcoal	Lyon-15271	3725 ± 30 BP	4152–3982	2203–2033 BC
	MGb05ch	155/160	Charcoal	Lyon-15272	3780 ± 30 BP	4245–4009	2296–2060 BC
	MGb06ch	210	Charcoal	Lyon-15273	4070 ± 30 BP	4800–4440	2851–2491 BC
MWb	**MWb03ch**	65/70	Charcoal	Lyon-13958	5120 ± 30 BP	5930–5751	3981–3802 BC
	MWb04ch	75/83	Charcoal	Lyon-15268	5310 ± 30 BP	6185–5995	4236–4046 BC
	MWb18ch	130	Charcoal	Lyon-14628	5590 ± 30 BP	6435–6303	4486–4354 BC
	MWb22ch	200	Charcoal	Lyon-15266	6140 ± 30 BP	7158–6951	5209–5002 BC
	MWb10ch	205	Charcoal	Lyon-13959	5905 ± 30 BP	6790–6663	4841–4714 BC
	MWb20ch	280	Charcoal	Lyon-14629	6485 ± 35 BP	7460–7320	5511–5371 BC
	MWb21ch	330	Charcoal	Lyon-13960	7180 ± 30 BP	8035–7945	6154–5987 BC
MAa	**MAa02ch**	225/230	Charcoal	Lyon-15283	1805 ± 30 BP	1822–1626	129–325 AD
	MAa03ch	295/300	Charcoal	Lyon-15284	1860 ± 30 BP	1870–1720	80–231 AD
	MAa05ch	410	Charcoal	Lyon-18411	4910 ± 35 BP	5715–5590	3766–3641 BC
	MAa06ch	440	Charcoal	Lyon-15285	5100 ± 30 BP	5917–5749	3968–3800 BC
AMb	**AMb02ch**	45	Charcoal	Lyon-13464	810 ± 30 BP	781–681	1169–1270 AD
	AMb02chbis	45/50	Charcoal	Lyon-14632	490 ± 30 BP	547–500	1404–1450 AD
	AMb03ch	65	Charcoal	Lyon-13465	615 ± 30 BP	656–550	1295–1401 AD
	AMb05ch	120	Charcoal	Lyon-13466	985 ± 30 BP	960–796	990–1154 AD
	AMb06ch	135/140	Charcoal	Lyon-14630	430 ± 30 BP	530–335	1421–1616 AD
	AMb07ch	160	Charcoal	Lyon-13467	1560 ± 30 BP	1530–1386	420–565 AD
	AMb08ch	170	Charcoal	Lyon-14631	765 ± 30 BP	732–668	1219–1283 AD
	AMb10ch	195	Charcoal	Lyon-13468	535 ± 30 BP	633–512	1318–1439 AD
	AMb11ch	220	Charcoal	Lyon-13469	515 ± 30 BP	625–506	1325–1445 AD
	AMb12ch	248	Charcoal	Lyon-13470	915 ± 30 BP	920–762	1030–1189 AD
	AMb13ch	265	Charcoal	Lyon-13471	880 ± 30 BP	908–729	1042–1222 AD
	AMb14ch	293	Charcoal	Lyon-13472	1275 ± 30 BP	1289–1150	661–800 AD
	AMb16ch	330	Charcoal	Lyon-13473	1785 ± 30 BP	1816–1618	129–345 AD

42 samples (almost 81%) was medium silts (9.36 to 16.26 μm). The large number of silty samples and the apparent homogeneity as demonstrated by the textural description should not mask the fact that overall, all the samples were very poorly sorted. This is consistent with colluvial sediments, especially slope deposits: the sediments were moved downhill and were not selected by size, shape, or gravity during their transportation (Friedman and Sanders, 1978; Chamley, 1987). These sediments tend to be less well sorted than alluvial sediments (Goldberg and Macphail, 2006; Cubizolle, 2009).

4.1.2 Organic matter and calcium carbonate content

In all three sections studied, organic matter content was consistent and relatively low (< 10%), ranging from 1.9% (in AMb) to 9.6% (in MWb). Similarly, calcium carbonates contents were very low, between 0.6% (MAa) and 12.8% (MWb). Overall, the coarser the sediments, the lower the calcium carbonate and organic matter contents. In all three sections, peak organic matter contents corresponded to higher fine sediment content. This good apparent correlation between grain size and organic matter content could mean that the organic matter was transported with the sediments rather than developing *in situ*. The combined observation of grain size and carbonate curves suggests that the carbonates are more probably of clastic origin and were transported with the sediments and/or result from erosion (denudation, transportation, deposition) of the substratum.

4.2 Chronostratigraphic studies

In this subsection, we present the chronostratigraphic observations and results for each site from upstream to downstream. The stratigraphy is described according to the facies description recorded during field work: as we did not reach the bedrock when studying the sections, numbering is from top to bottom, as done during field work, to leave open the possibility of taking deeper samples in a future campaign.

4.2.1 The Mengangebit section b (MGb)

In Mengangebit, the MGb section was studied in the MG cone described below. The MGb section is a 230 cm thick

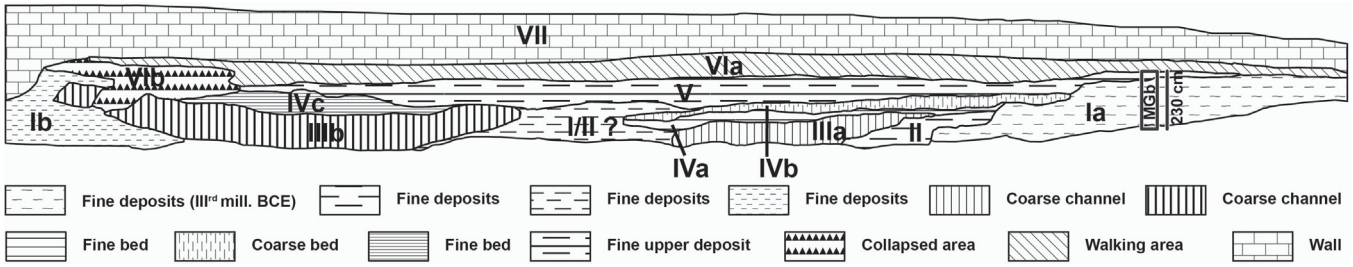

Fig. 9. Stratigraphic sketch of the Mengangebit cone.
Fig. 9. *Croquis stratigraphique du cône de Mengangebit.*

section located on the right side of the cone when facing it (Figs. 7 and 9), where very fine deposits of clayey appearance, silt, sand and stony beds alternate (Fig. 10). The whole section is dark brown or reddish. The beginning of the observable sedimentation is marked by a coarse deposit (SU07), indicating competent flows prior to 4800–4440 cal. BP (Fig. 10). It is followed by a phase of fine deposition, around 4800–4440 cal. BP, during which pedogenetic processes began (dark homogeneous silts, SU06). An erosional contact marks the limit between this and the following 35-cm thick unit, comprised of interstratified silty layers and gravelly lenses (SU05). This phase ends with a very fine deposit dating from 4245–4009 cal. BP (SU04). Then, after what appears to be the start of a pedogenetic process, there is a long phase of fine deposition interspersed with coarser beds (SU03). The abundant sand-silty matrix and the gravelly size of the coarser particles suggest muddy flows rather than a real torrential process. The two charcoals constraining the thin paleosol are chronologically consistent (MGb04ch is younger than MGb05ch), whereas the next two ages are older, (4347–4090 cal. BP and 4245–4009 cal. BP, see Fig. 10 and Tab. 1), and show chronological inversion. We cannot exclude the possibility that these date inversions within the same stratigraphic unit (SU03) are due to an "old wood" effect (Stouvenot *et al.*, 2013) or to stratigraphic contamination (Carcaillet and Talon, 2007; Pelling *et al.*, 2015), especially since the radiocarbon ages are very close and the charcoals were found not very far away from one another. A more probable hypothesis is the erosion of older deposits in the catchment, SU03 probably marking the resumption of erosion phenomena after a lull. Finally, the two top units (SU02 and SU01) are relatively coarse (the b axis of the pebbles reaching 10–12 cm) and mark a break with SU03 (SU02 in erosional contact). SU01 corresponds to the depth currently affected by ploughing. This section shows that five phases succeeded between 4800–4440 and 4152–3982 cal. BP. After a first stage, a phase of incision seems to have occurred at the end of this period, followed by a short period of stability, as suggested by the thin pedogenic layer. Aggradation then resumed and a last phase, undated, is marked by clearly coarser sediments.

These results tend to show that, during this period which lasted almost a millennium, the catchment was relatively sensitive to erosion and the thresholds of process initiation were quite low. It is difficult to determine the triggering factors precisely insofar as this site did not provide archaeological or palaeoecological information.

The processes observed in the MGb section must also be viewed in the stratigraphic context of the cone.

4.2.2 The Mengangebit cone site

In cross section, the Mengagebit cone shows several stratigraphic units. On the left and right margin and in the centre of the accumulation, mainly fine deposits appear to constitute the oldest part of the cone (I and II, Fig. 9). This deposit is notched by paleochannels filled by a complex detrital body, in which several successive phases of erosion and filling can be observed. The cone seems to be mainly the result of the accumulation of sediment at the outlet of two small tributaries on the slopes and which are visible in Figure 7.

All the steps described here with Roman numbers appear in Figure 9. The fine sediments (I and II) were deposited first, indicating rather regular and low energy colluvial processes from the slope and/or the two small tributaries. The MGb section (between 4800–4440 and 4152–3982 cal. BP) was studied in one of these fine deposits (Ia) (see above). The following events are therefore assumed to have occurred after this period. The fine deposits were notched for the first time, but the channel was subsequently filled by other fine deposits (II). Fine deposits were also present in the central part of the main paleochannel but without dating, it is difficult to confidently attribute the central fill to the first or second fine phase, which explains the question mark (I/II?). Two ablation episodes then occurred, corroborated by two channels filled with coarse material including blocks and pebbles in a fine matrix, mostly visible in the central part (IIIa and IIIb). Given their direction, it is likely that these incisions were caused by the above-mentioned tributaries and filled with coarse material derived from the slopes. According to the results of dating the MGb section, it is likely that this phase of incision and backfilling occurred after the more recent dated period (4152–3982 cal. BP). The clear coarsening of the grain in the detrital deposits and the torrential aspect of the two paleochannels (IIIa and IIIb) strongly suggest that biostatic conditions did not prevail in the cone drainage area at that time. One can also assume that this change is the consequence of opening the vegetation, but it is impossible to determine if this was only due to land clearing by groups of humans or is also the result of a change from a wet to a drier climate which occurred approximately 4000 years ago. The accumulation was capped by fine colluvio-alluvial deposits (IVa and IVc), one of which was covered by a coarse bed (IVb). The entire

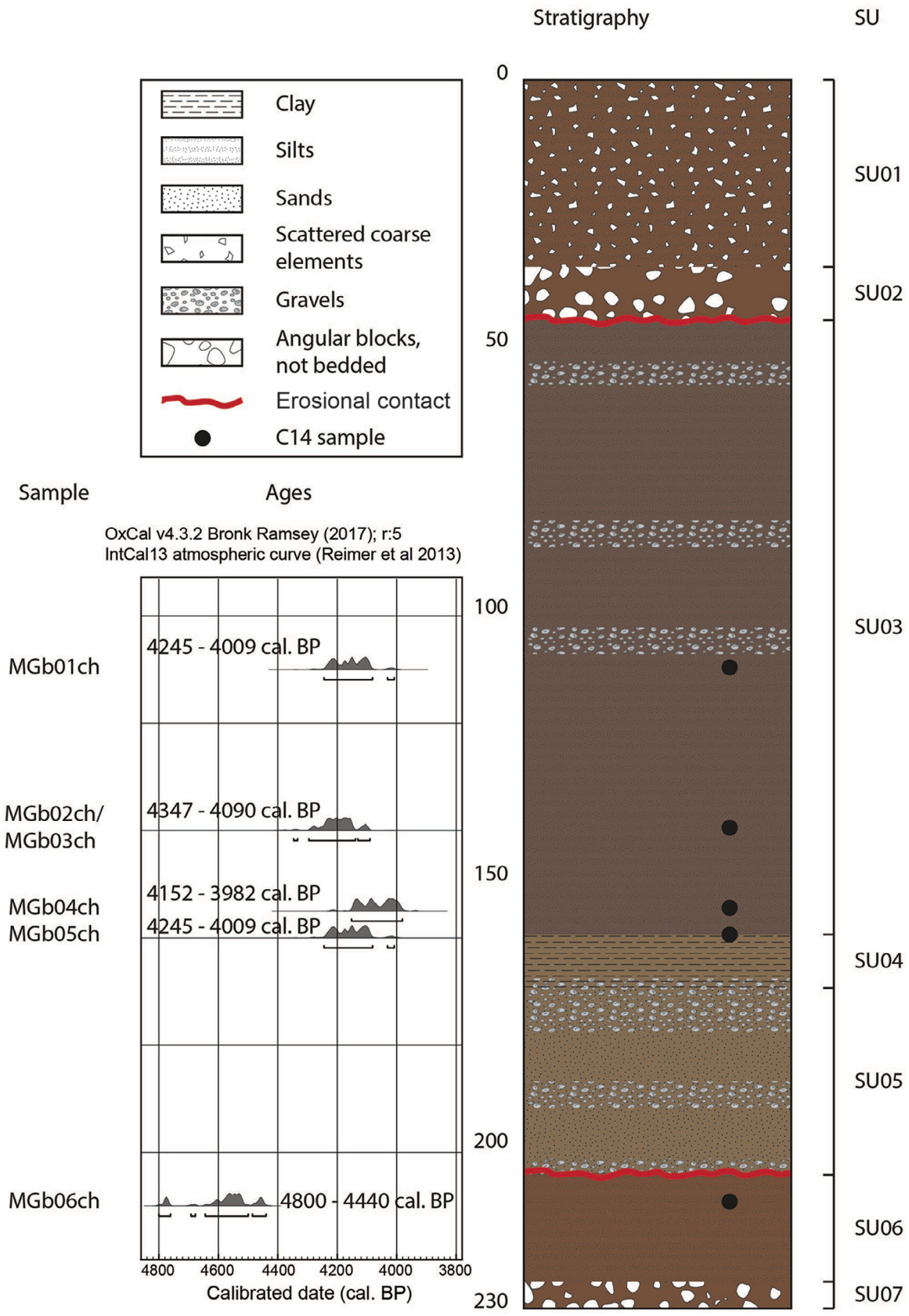

Fig. 10. Ages and depths of the MGb section.
Fig. 10. *Âges et profondeurs de la coupe MGb.*

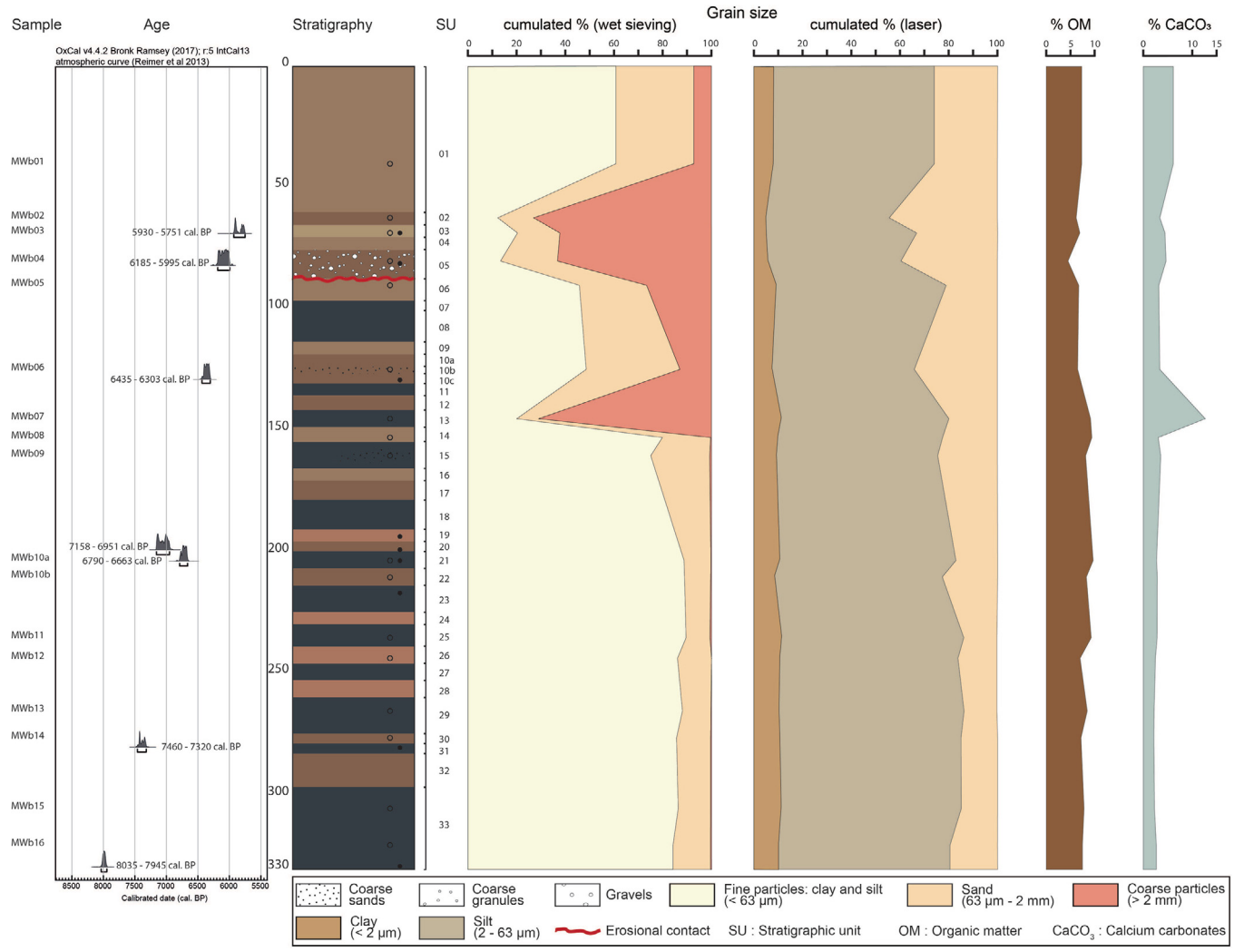

Fig. 11. Ages, stratigraphy and sedimentology of section MWb.
Fig. 11. *Âges, stratigraphie et sédimentologie de la coupe MWb.*

cone thus appears to have been covered with a fine deposit (V). Finally, the whole accumulation was eroded into a detrital terrace along the stream by longitudinal erosion of the Mengangebit valley floor. Today, only a few fragments of the initial fill remain on each bank, including the cone studied here. Recently, following the development of agricultural terraces, the upper deposit was levelled (VIa) and one area collapsed (VIb). Finally, hydro-agricultural development included the construction of a wall to support the upstream terrace (VII). It is likely that this terracing for agriculture at least partially contributed to the preservation of the cone.

4.2.3 May Weini site – section b (MWb)

This section is characterised by a mostly fine dark material. The accumulation of very silty sediments continues almost throughout the section, except for a few beds containing small coarse particles deposited in erosional conditions. From bottom to top, dark brown layers alternate with light brown layers, followed by brown layers alternating with greyish layers and finally a homogeneous dark grey layer (Fig. 11).

In this section, wet sieving revealed a clear contrast between the lower part, mainly composed of fine-grained particles (clay and silt, < 63 µm, clearly dominating the distribution ranging from 75.1% to 89.8%) and the upper part, from SU13 to the top, in which the coarse fraction (> 2 mm) accounts for between 12.8% and 73%, and fine particles for less than 50% (Fig. 11). These five coarser sediment samples are trimodal, with more sand and less silt than the others, two are bimodal, and most of the others are unimodal (Fig. 12). Nevertheless, the main mode of all samples of MWb is in medium silts.

Among the granulometric indices (sorting, skewness, and kurtosis), sorting ranged from 4.25 to 6.64, showing the samples to be very poorly sorted and indicating that colluviation was the main process of transport and deposition. Sorting remained similar throughout the distribution of most of the samples, as indicated by kurtosis: 14 samples are mesokurtic; only three are platykurtic, indicating better sorting in the "tails" of the distribution than in the central zone. The skewness index points in the same direction: eight samples are symmetrical (among which five are unimodal, indicating rather

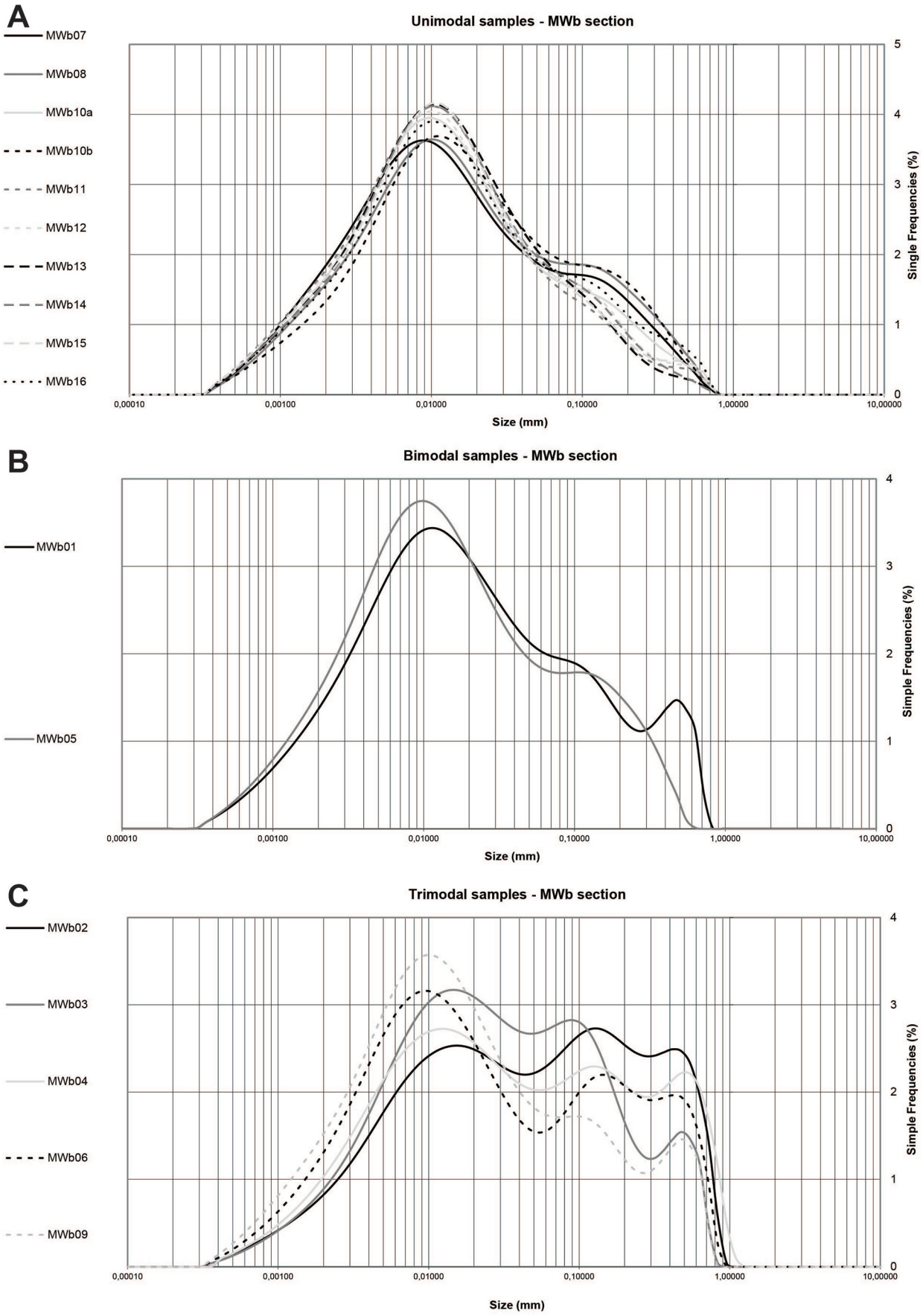

Fig. 12. Grain size curves, MWb section. A: Unimodal samples; B: Bimodal samples; C: Trimodal samples.
Fig. 12. *Courbes granulométriques, coupe MWb. A : échantillons unimodaux ; B : échantillons bimodaux ; C : échantillons trimodaux.*

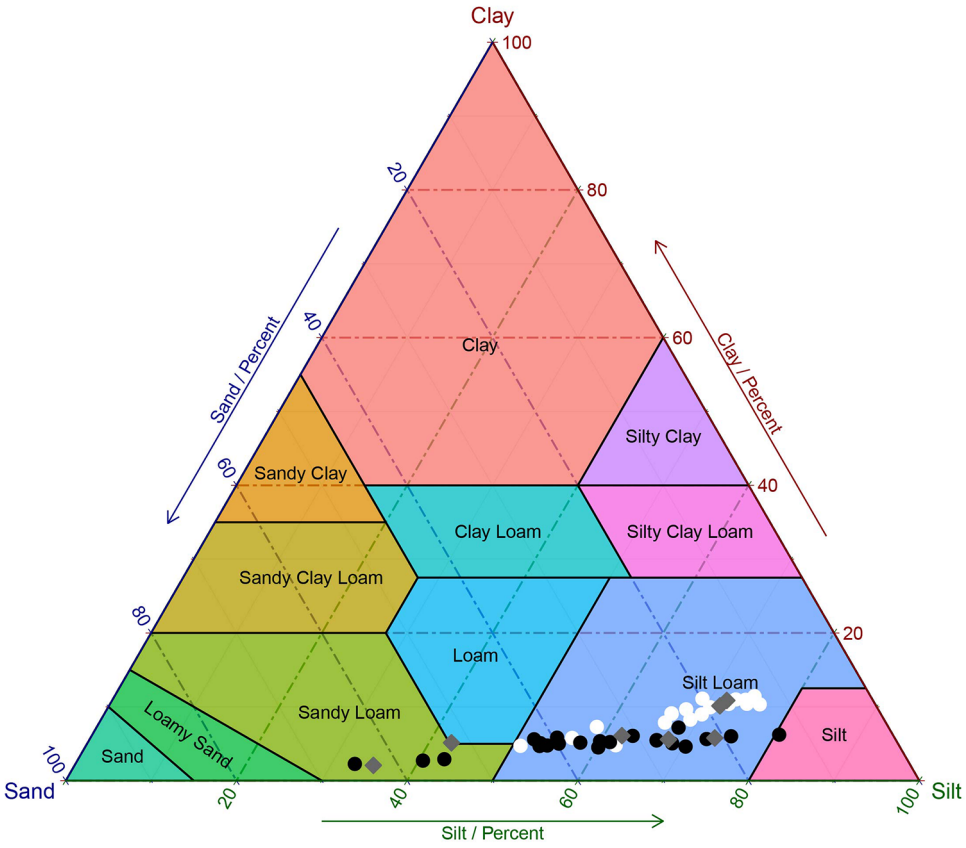

Fig. 13. Triangular diagram of the laser granulometry for MWb (white), AMb (black) and MAa (grey). Drawn using R language, and the packages ggtern (Nicholas Hamilton) and plyr (Hadley Wickham).
Fig. 13. *Diagramme triangulaire des résultats de granulométrie laser des coupes MWb (en blanc), AMb (en noir) et MAa (en gris). Réalisé en langage R, à l'aide des paquetages ggtern (Nicholas Hamilton) et plyr (Hadley Wickham).*

good distribution of fine sediments) and nine are coarse or very coarse skewed (negative-skewed), meaning that their distributions have a "tail" of coarse sediments.

In this section, organic matter and calcium carbonates contents were relatively low (9.6% and 12.8%, respectively), but nevertheless the highest amongst the study sites. The mean organic matter content in the section was 7.5%. The figures show a slight decreasing trend from the bottom to the top (organic matter contents ranging between 4.5% and 9.6%), suggesting a link with mean grain size, with the grain size increasing towards the top of the section. This could mean that the organic matter was transported with the sediments rather than formed *in situ*. Furthermore, the peak in carbonates corresponds to a peak in coarse material (Fig. 11): carbonates could originate from the geological composition of the area ("dolomite interbedded with slate", Kazmin, 1976, Fig. 2). Combined observation of grain size and carbonate curves suggests that carbonates are probably of clastic origin and were transported with the sediments and/or result from the degradation of the substratum. Locally, they could also originate from erosion of the tuffaceous concretions that formed at the mouth of small springs at the foot of the slopes of this catchment.

The ages of this accumulation range from 8035–7945 cal. BP to 5930–5751 cal. BP (Tab. 1). The dates are distributed in the section in chronological order, except for an inversion between samples MWb10ch (6790–6663 cal. BP, 205 cm below the surface) and MWb22ch (7158–6951 cal. BP, 200 cm).

Overall, sedimentological data and ages determined on the charcoal fragments show undisturbed sedimentation from 8035–7945 cal. BP to 5930–5751 cal. BP (Tab. 1 and Fig. 11). For this reason, it was possible to distinguish two groups in the accumulation.

The first group is comprised between the SU33 and the SU14 and accumulated from 8035–7945 cal. BP to 7158–6951 cal. BP. The fine grain size and the slightly higher organic matter content of these deposits could be linked to an environment where the slopes are covered by relatively dense vegetation, which supposes wet climatic conditions and probably the absence of heavy rainfall events. The higher organic matter content could be explained by later migration in the accumulated soil, by the deposition of organic sediments, or by the development of vegetation on the sediment accumulation under wet conditions. The charcoals have not been identified, so one cannot be certain, but the chronological inversion between MWb10ch and MWb22ch could be the result of stratigraphic contamination or of an "old-wood" effect (Stouvenot *et al.*, 2013), if the dated taxa of MWb22ch were much longer lived than the taxa of MWb10ch (for example, *Podocarpus falcatus vs. Juniperus procera*, *cf. infra* in the charcoal determination section). The chronological

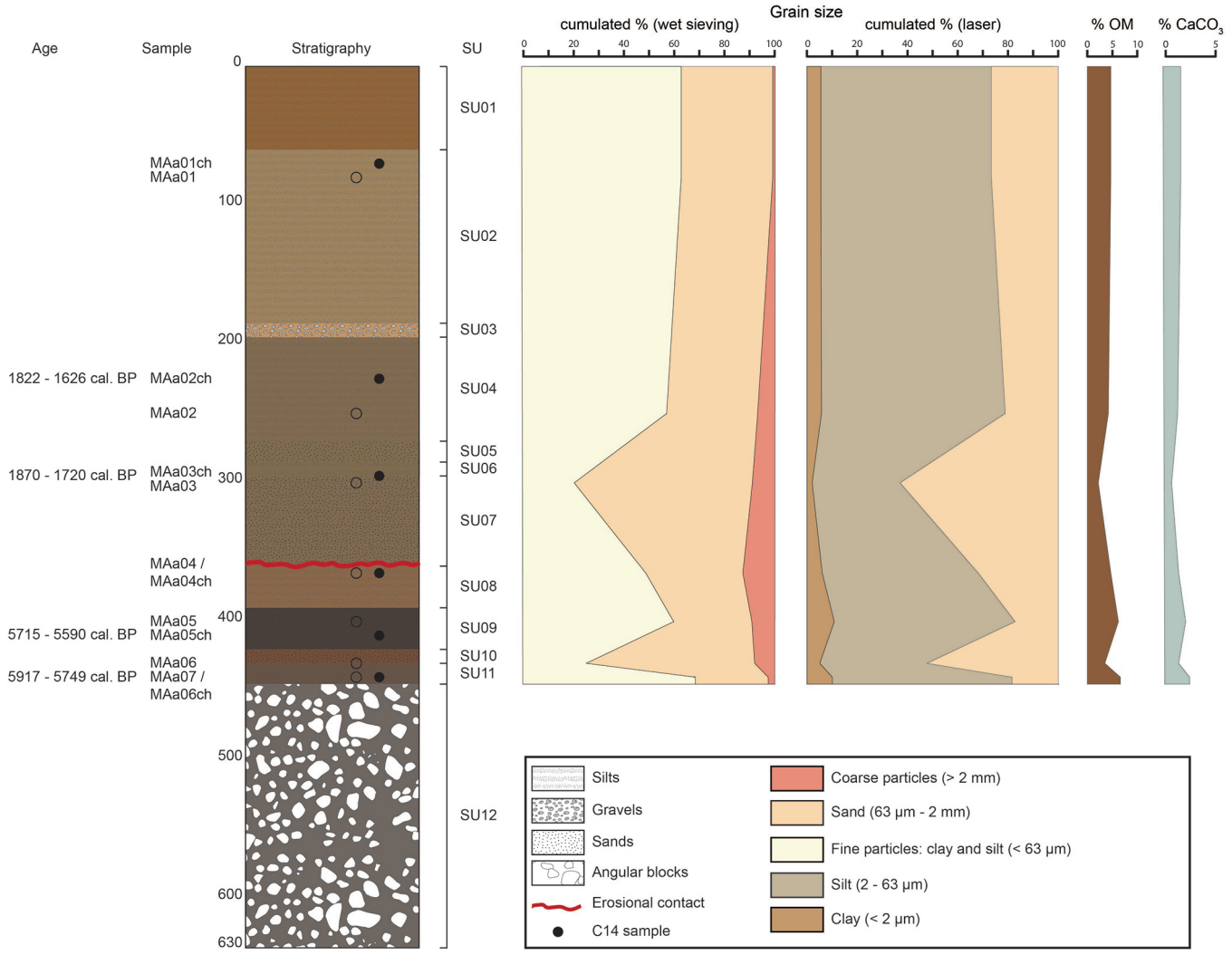

Fig. 14. Ages, stratigraphy and sedimentology of section MAa.
Fig. 14. *Âges, stratigraphie et sédimentologie de la coupe MAa.*

inversion could also be due to reworking of older charcoals in the watershed.

The second group encompasses SU13 to SU01, with ages ranging from 6435–6303 to 5930–5751 cal. BP. The colour of the sediment tends to become paler, perhaps an indication of an increase in the sedimentation rate which prevented organic matter enrichment. This group contains the coarsest samples of the section (Figs. 11 and 13), that have the higher sand content (laser granulometry, Fig. 11) and lower organic matter and clay contents (4.7% to 9%). The presence of sand and gravel beds (SU10b and SU05), with no apparent deposition structure (no bedding) suggests a change in the functioning of the catchment area, with more concentrated flows and higher energy. The SU05 is the coarsest layer in the section and dates from 6185–5995 cal. BP. Its erosional contact with the underlying layer suggests that, at that time, some events may have had sufficient energy to rework sediments previously deposited in the thalweg. This could be related to changes in the surface of the catchment, like reduced vegetation cover, or to changes in meteorological conditions, like increased rainfall, factors that are more favourable to concentrated runoff and motion of coarser particles on slopes. Furthermore, the position of the section far upstream in the catchment could explain the downstream discharge of fine particles during high energy episodes. It is possible that the chronological inversion represented by the MWb22ch sample corresponds to the beginning of these changes, if interpreted as erosion of older deposits.

4.2.4 May Ayni site – section a (MAa)

In this site, a well dug in the sedimentary fill by a farmer allowed us to observe a 630 cm thick sedimentary accumulation (Figs. 5 and 14) resting on the bedrock that was cut by the farmer to a depth of 185 cm. The bedrock belongs to the Tsaliet Group ("intermediate and basic lavas, greywacke, tuffaceous slate, phyllite, agglomerate and rhyolite") (Kazmin, 1976). Its composition is summarised by Chernet (1988) as "precambrian low-grade metamorphics" (Fig. 2). Granulometric analyses

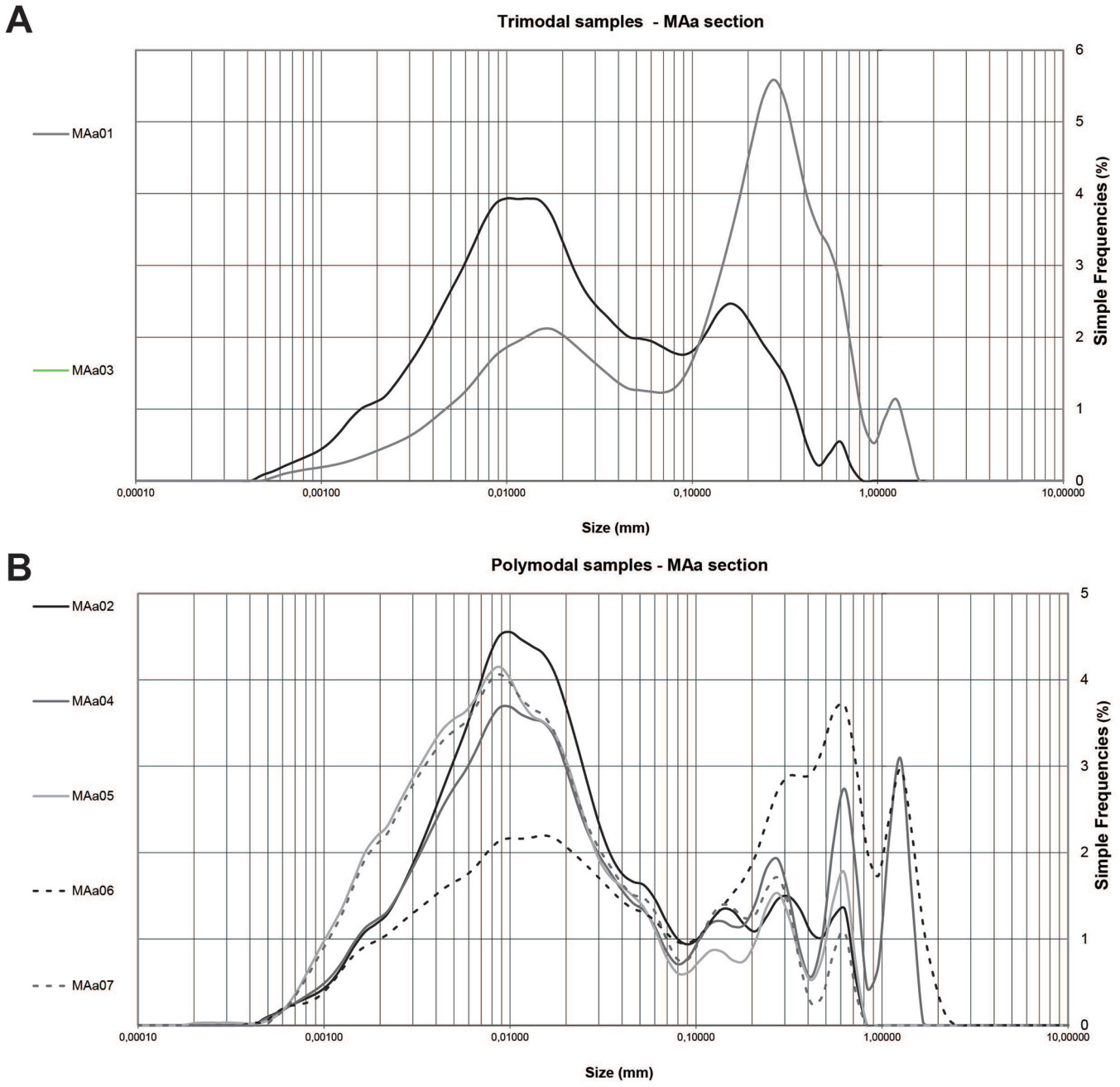

Fig. 15. Grain size curves, MAa section. A: Trimodal samples; B: Polymodal samples.
Fig. 15. *Courbes granulométriques, coupe MAa. A : échantillons trimodaux ; B : échantillons polymodaux.*

revealed the samples to have complex grain size distribution, with at most only two trimodal samples, the five remaining being polymodal, with at least four recognizable modes (Fig. 15). In this site, sediments have the highest (poorest) sorting indices (ranging from 4.96 to 8.71) of all the samples analysed. Organic matter and calcium carbonate contents decreased from the bottom to the top (Fig. 14). According to *in situ* observations and to the results of analyses, the sedimentary accumulation can be divided into four groups.

First, resting on the bedrock surface, SU12 is a 185-cm thick fill comprised of boulders, blocks, and pebbles, which represents a unique case in our corpus of sites. It was not possible to sample this part, nor to date it. Nevertheless, SU12 rests under SU11, dated from 5917–5749 cal. BP (Tab. 1), so it can be assumed to have been deposited before this date. As can be seen in Figure 5, this first group has three sequences. The first sequence is composed of rounded tilled boulders and blocks, with poor to no matrix. The second sequence is made of smaller rounded elements (pebbles), in a matrix of fine particles (probably sands) with no well-organized bedding. Towards the top of this unit, the elements are finer (pebbles, gravels) and the fine and silty matrix is more abundant. This last layer follows a lateral slope that is steeper than the underlying beds. The apparent absence of erosional contact

between the layers suggests that this detrital fill is related to different torrential cones that coalesce here (the site is close to a confluence), or to a mobile braided channel on the valley floor. The absence of matrix and the grain size indicate high energy sedimentary fluxes and the rounded particles suggest characteristics closely resembling those of a torrential stream. This could be linked with abundant rainfall events or short period of concentration of runoff in the catchment.

The second group (SU11 to SU08) is heterogeneous, composed of alternating fine and coarser sediments deposited after 5917–5749 cal. BP. The contact with SU12 is depositional, SU11 capping the upper coarse bed with a layer of silt. SU10 is formed of very thin interstratified layers of sands and silts. It has a mode of very coarse sands (1352.2 μm) indicating colluvio-alluvial processes in which particles were probably transported over short distances, and derive from multiple local sources of sediments, like slopes or small catchments located near this site. SU09 and SU08 present no clear alluvial bedding but rather a mix of different grain sizes, visible through the very bad sorting of the samples. The samples are also coarse (SU09) and very coarse skewed (SU08): this "tail" of coarse sediments suggests mixing of sediments from different sources, particularly visible in the SU08 where the silty matrix contains sparse gravels or small pebbles (Fig. 14). This group marks a transition from alluvial to colluvial processes.

A stratigraphic discontinuity separates this sequence from the third group. This could explain the apparent break in deposition rates: less than 200 years elapsed between MAa06ch and MAa05ch, separated by 30 cm, while a very long period – more than three millennia – elapsed between MAa05ch and MAa03ch, whereas the charcoal fragments are separated by only 110 cm. On the other hand, less than a century separated the two samples MAa03ch and MAa02ch, which are 70 cm apart (Fig. 14 and Tab. 1). At the base of this group, SU07 comprises many sandy lenses and layers in a silty matrix. SU06 and SU05 are clearly separated silty and sandy layers. These sedimentary facies suggest the thalweg was swept by moderate energy sheet floods.

The fourth group ranges from SU04 to SU01 and is characterised by more homogeneous sedimentary facies from 1822–1626 cal. BP onwards. SU04 and SU02 are formed by coarse skewed silts ("tails" of coarse sediments, mainly sands, in the distribution). They are separated by a thin sandy-gravely bed (SU03) marking the interruption of the fine sedimentary aggradation by a higher energy event. The sequence ends with a silty accumulation comparable to SU02 but includes traces of ploughing in its upper part. Organic matter and carbonates reveal no interpretable trend in this part of the fill.

Radiocarbon dating revealed two groups of ages, about 6000 years ago (MAa06ch and MAa05ch) and about 2000 years ago (MAa03ch and MAa02ch) (Figs. 14 and 16 and Tab. 1). Given the available age data, we only have a *terminus ante quem* for the torrential deposits covering the substratum. We can assume that the conditions that prevailed when these layers were deposited ended at the latest around 5917–5749 cal. BP when the fine-grained deposits covered the boulder units, suggesting that the local environment evolved towards biostatic conditions, providing only fine particles. Moreover, here, the valley seems to be too narrow for the torrential channels to migrate laterally without the influence of high-energy fluxes that are still perceptible in the sedimentation in the rest of the valley floor, thus supporting the hypothesis of an environmental change. Nor is it possible to set a chronological limit to these colluvio-alluvial dynamics. The long time gap between the two groups corresponds to the stratigraphic discontinuity observed in the sequence, and suggests a vertical incision of the channel or the erosion of older deposits. Given that 70 cm separate the two samples MAa03ch and MAa02ch for a time gap of less than a century (Tab. 1 and Fig. 16), one can assume a relatively rapid sedimentation rate. Aggradation continued after 1822–1626 cal. BP (MAa02ch), but the absence of dating at the top of the section prevents the precise determination of the rhythms of the valley filling. No trace of artefacts or buildings was found, and the influence of local human settlements (corresponding to the Aksumite times) is not directly perceptible in this section.

4.2.5 Ambare valley site (AMb)

In the Ambare valley, the river channel entrenchment offers numerous observation sites of sedimentary fills. The bedrock was not reached during the preparation of the section because the water table, located about 30 cm below the bottom of the channel, made it impossible to dig deeper. Nevertheless, the riverbed is deeply incised all along this valley and frequently reveals bedrock outcrops so it is likely that this section represents almost the entire thickness of the alluvial fill. The selected section is a 355-cm thick alluvial accumulation, where fine sediments predominate. Almost all the samples (15/18) belong to the silt loam group (Fig. 13). AMb is the section with the greatest number of dated samples: the 13 ages range from 1816–1618 cal. BP to 530–335 cal. BP and shows numerous stratigraphic inversions (Fig. 17).

It is possible to distinguish two main parts: a 130-cm thick light grey and blueish grey base (SU13d–SU13a) and an upper light brown and yellowish-brown part (SU12–SU01).

The lower part of the section (SU13d–SU13a) is composed of four stratigraphic units of fine, light grey to blue grey sandy silts (Fig. 18) in which there is no clearly visible stratification nor erosional contact between layers but rather progressive transitions of textural characteristics. Grain size analyses showed that sediments are bimodal (silts with a secondary mode of sands or sands with a secondary mode of silts) (Fig. 19); their very poor sorting and the mainly coarse skewness of their distribution suggest a mixture of sediments of various origins, with a preponderance of large-calibre elements (Friedman and Sanders, 1978). Combined with the almost total absence of coarse particles and "normal" sedimentation (no stratigraphic inversion), these characteristics suggest the sediments were deposited under a regular, low-energy hydrological regime and are likely overflow silts in an alluvial plain. Indeed, given the longitudinal slope of the thalweg (0.02 m/m), larger particles such as blocks or pebbles could have been transported and deposited here if the flow energy (*i.e.*, the discharge) of this small mountain stream had been sufficient. Their absence in the stratigraphy suggests that the energy of the watercourse was insufficient for their transport (Gob *et al.*, 2010). Besides, as the bottom of this valley is very narrow and the substratum is only covered by a thin alluvial sheet, the lateral migration as well as the entrenchment of the river channel could only have been very

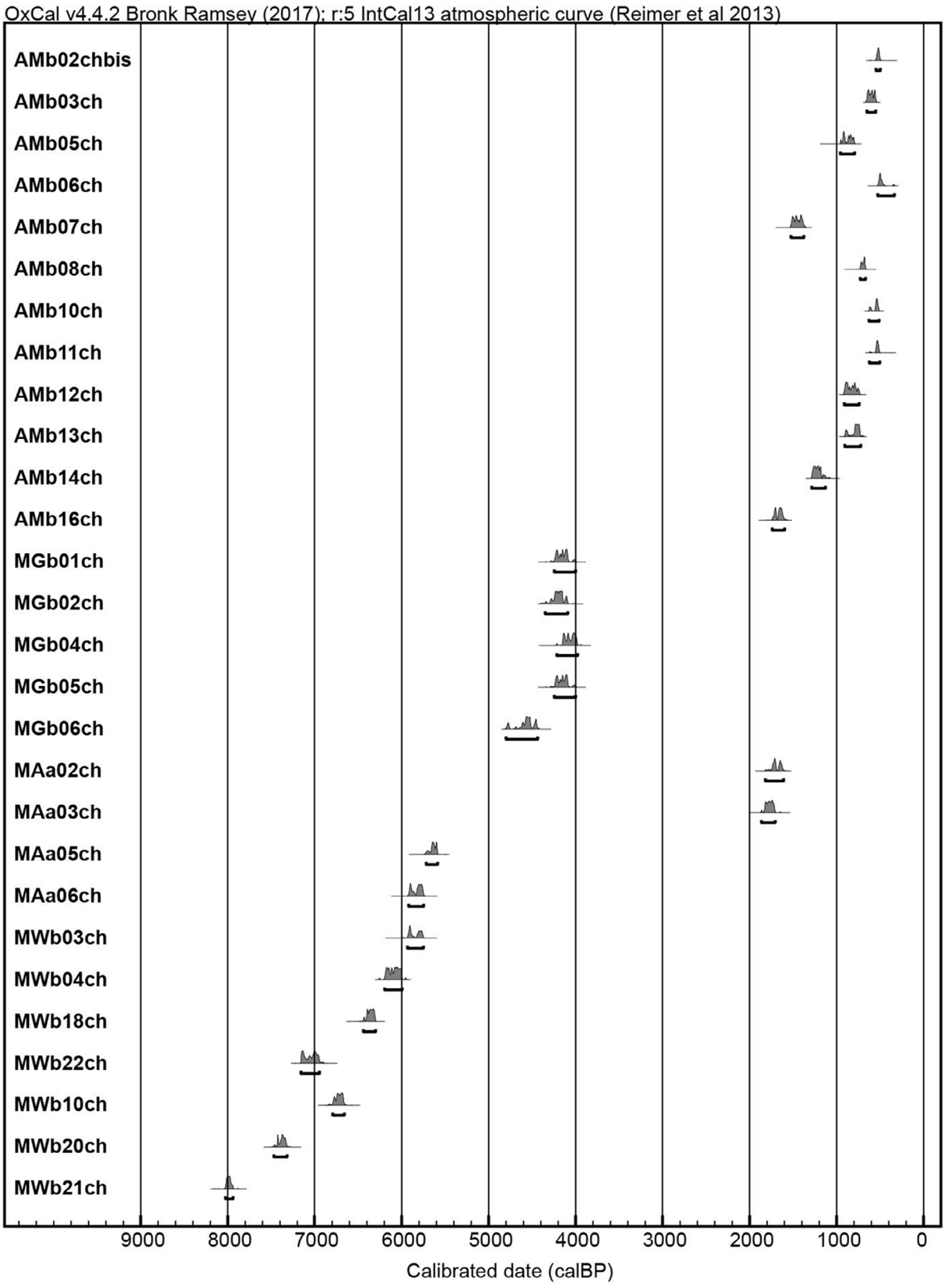

Fig. 16. Synthetic presentation of all dated samples in the study. Plotted with OxCal v.4.3.2 (Bronk Ramsey, 2017) and calibration curve by Reimer *et al.* (2013).

Fig. 16. *Présentation synthétique de tous les échantillons datés de cette étude. Représentation avec OxCal v.4.3.2 (Bronk Ramsey, 2017) et courbe de calibration de Reimer et al. (2013).*

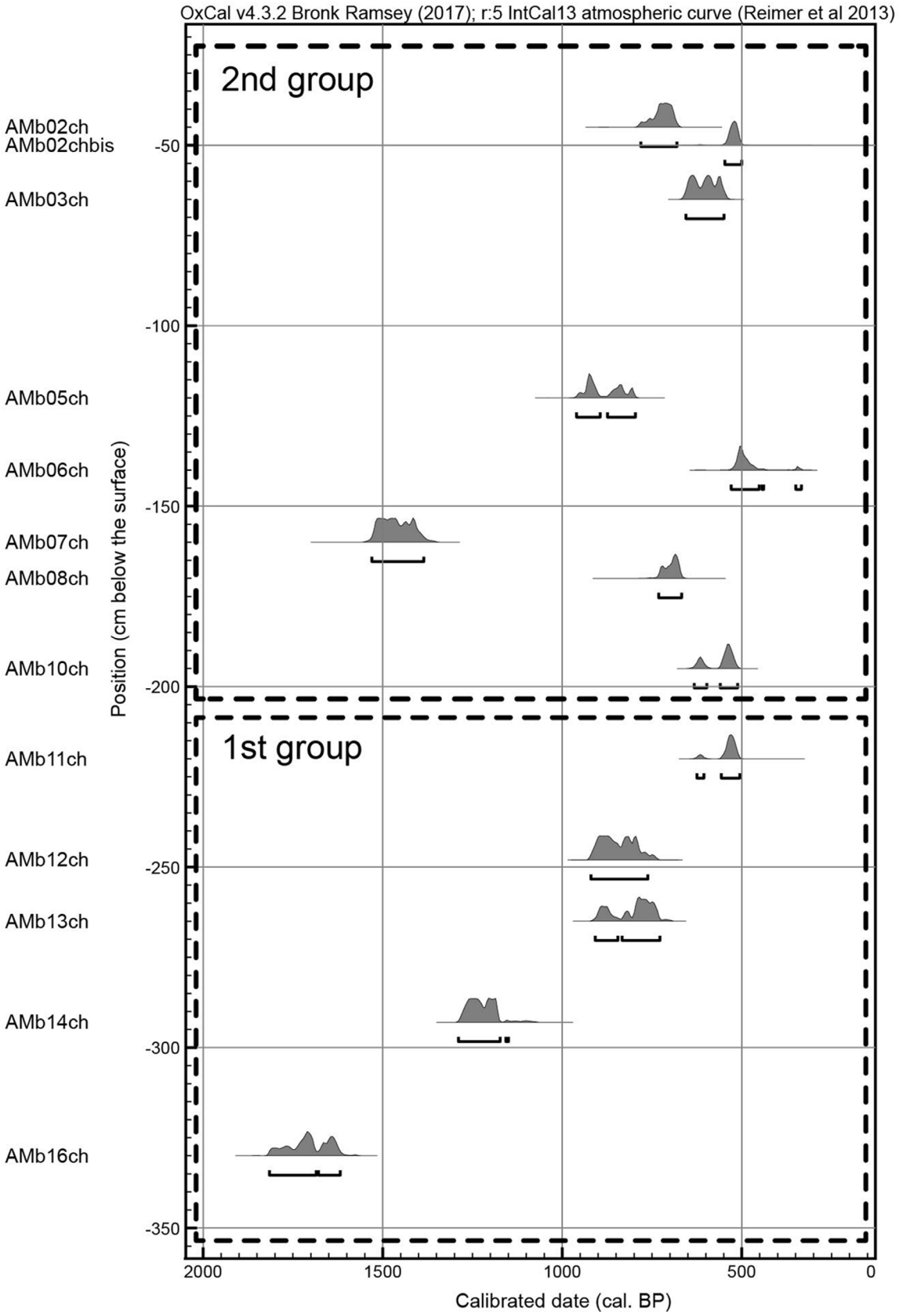

Fig. 17. Ages and depths of section AMb.
Fig. 17. *Âges et profondeurs de la coupe AMb.*

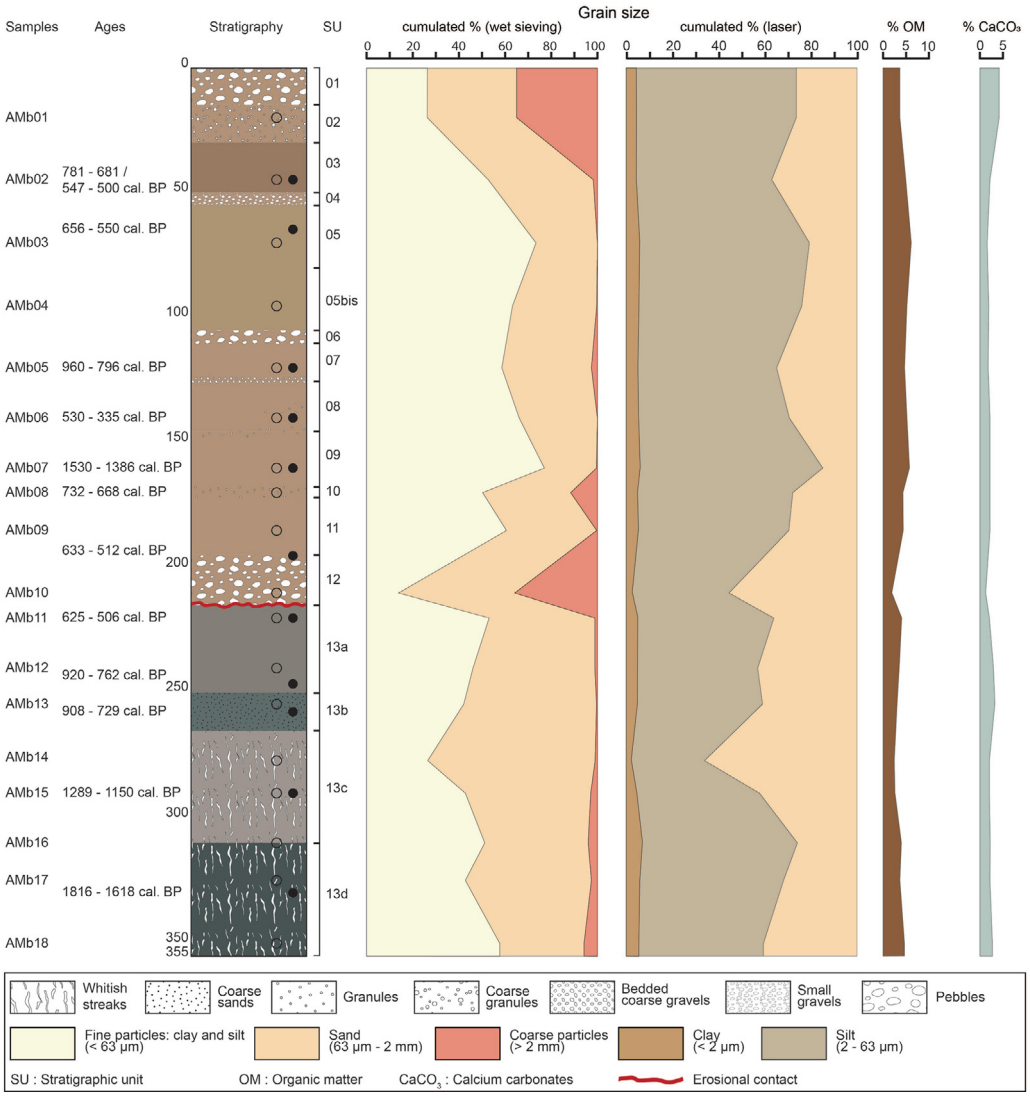

Fig. 18. Ages, stratigraphy and sedimentology of section AMb.
Fig. 18. *Âges, stratigraphie et sédimentologie de la coupe AMb.*

limited so that evidence of high-energy events would inevitably be detectable in stratigraphy if they existed. The colour and aspect of the sediments show that they underwent later evolution, likely under hydromorphic conditions. This shows that the riverbed bottom and the permanent water-table were subsequently at a higher elevation than today. Radiocarbon ages show that these sedimentary units were deposited between 1816–1618 cal. BP and 625–506 cal. BP, *i.e.*, at moderate aggradation rate (10 cm/century). As the lower part of the valley fill has not been excavated, the start of these dynamics remains unknown. Nevertheless, it should be noted that the ages are consistent and in chronological order (Fig. 18). The apparent age inversion between AMb13ch and AMb12ch could be explained by stratigraphic contamination (Carcaillet and Talon, 2007; Pelling *et al.*, 2015) or because the dated fragment corresponds to heartwood of a long-lived species such as *Podocarpus falcatus* (see charcoal identification below).

An erosional contact marks the limit of the upper part of the section (SU12-SU01). The rupture is also apparent in the organic matter and calcium carbonate rates, which are lower than in the rest of the section (Fig. 18). This sequence begins by a 15-cm thick layer of gravels, pebbles, and small fluvial blocks (SU12), followed by irregular alternation of silty and sandy-gravelly layers (SU11 to SU01). Silty units, SU11, SU09, SU08, SU05bis and SU05, are quite homogeneous and finer than the lower sequence sediments (Fig. 18) and have a higher organic matter content. The mainly coarse skewness of the samples indicates enrichment of the silts by coarser elements. The coarser layers (SU10, the base of SU07, SU06, SU04, SU02 and SU01) are often thin deposits of gravels, or lenses of coarse sands in a silty matrix. Only two units (SU06 and SU01) contain pebbles or small fluvial blocks. These sedimentary features suggest an aggradation process during which alluvial deposits with different granulometry overlapped or interlaced, depending on variation in the flow or on

the position of the riverbed in the floodplain. Between 633–512 cal. BP and 530–335 cal. BP, events of low competence (not very concentrated, average rainfall) alternated with more powerful events (concentrated rainfall, floods, torrential episodes). This process seems to have started around 633–512 cal. BP, if we consider the discontinuity represented by the SU12, well constrained, both on the bottom and the top, by two very close ages. The age of another available sample (SU08) suggests that the process could have lasted at least up to 530–335 cal. BP. Under this hypothesis, it is possible to roughly evaluate the aggradation rate between SU12 and SU08 at 45–80 cm/century, which is clearly higher than that of the lower sequence. It is not possible to give an estimation for the top of the section as the two last SU do not contain exploitable data. Indeed, they correspond to the layer that was regularly affected by ploughing, which may explain why the stratigraphy is disturbed and why pebbles, coarse gravel and finer material can be found there with no apparent structure.

Nevertheless, the great number of charcoals dated between about 8000 and 6000 years ago and the frequent chronological inversions suggest that strong erosion affected the hydrological basin at that time or shortly thereafter, releasing sediments and charcoals that were previously stored upstream, either on the slopes or in the headwater thalwegs. The higher organic matter contents may also confirm the hypothesis of the erosion of soils, whether cultivated or covered by spontaneous vegetation. This sequence is evidence for the probable effects of environmental changes in this area. For the same reasons as in the lower sequence, one can assume moderate energy fluvial processes prevailed. Pebbles with a *b* axis >10 cm are extremely rare in the stratigraphy, and a silty matrix dominates. Given that coarse particles (gravels, pebbles) were found at all depths in the sequence, it is likely that the channel was not very deeply incised and was of the sandy braided type. In the absence of any chronological data in the upper part of the section, the *terminus post quem* of this dynamic remains unknown, as well as the beginning of the incision which led to the entrenchment of the current channel.

To sum up, the Ambare section provides information about the last two millennia and shows that an environmental change occurred approximately 6000 years ago, resulting in an increasing rate of aggradation on the valley floor, associated with a slight increase in flow competence compared to the previous period.

4.3 Results of charcoal determination

Charcoals in the MWb and AMb sections were identified, as these sections yielded samples that were large enough to be analysed.

The only identified sample from the MWb section, MWb07, was located 145 cm below the surface of the section (Fig. 11). The SU in which it was found has not been dated directly, but is framed by two dated SU: below, SU21 (MWb10ch, 205 cm below the surface), with an age of 6790–6663 cal. BP; above, SU10c (MWb18ch, 130 cm below the surface), with an age of 6435–6303 cal. BP (Tab. 1). It can therefore be assumed that the age of the sample of charcoal is within these two chronological ranges. However, it was much degraded and was only identified as an angiosperm.

The charcoal fragments in the AMb section are more recent and could be identified more precisely. Two samples, AMb13ch (265 cm below the surface, 11 fragments studied) and AMb12ch (248 cm below the surface, 2 fragments studied, see Fig. 18), were analysed, out of a total of 13 fragments. Almost all the identifications (12/13) referred to the genus *Juniperus* sp., of which the only known species in Tigray is *Juniperus procera* Hochst. ex Endl. (Bekele-Tesemma and Tengnäs, 2007; Friis *et al.*, 2010), a medium-sized tree that can reach 20 to 25 m in height, exceptionally 40 m, with a trunk ranging from 0.8 to 2 m in diameter (Farjon, 2005; Couralet and Bakamwesiga, 2007; El-Juhany, 2014). It is one of the dominant species in the evergreen forests of Ethiopia and in the Ericaceae formations between 1200 and 3500 m asl, that can survive in dry conditions (Bekele-Tesemma and Tengnäs, 2007). It has a lifespan of about 100 years, sometimes up to 200 years (Couralet and Bakamwesiga, 2007; El-Juhany, 2014). The wood of this species is widely used for carpentry and construction (Maydell, 1990; Ruffo *et al.*, 2002; Bekele-Tesemma and Tengnäs, 2007) and is also used in traditional medicine (Ruffo *et al.*, 2002) and for its essential oils.

One of the two fragments identified at AMb12ch was attributed to the genus *Podocarpus* sp., a conifer whose only known species in Tigray is *Podocarpus falcatus* (Thunb.) R.Br. ex Mirb. (1825) (synonym *Afrocarpus falcatus* (Thunb.) C.N.Page). This is a 45–60 m tall conifer (Farjon, 2005), which grows in low, semi-humid forests at altitudes of 1400–2900 m asl, often associated with *Juniperus procera* (Friis *et al.*, 2010). Some of the oldest individuals found in South Africa today could be 1000–1500 years old[1]. Its wood is used as fuel or timber, its fruits are edible, and its seeds and bark are used in traditional medicine (Bekele-Tesemma and Tengnäs, 2007). The analyses did not show whether the fragments of *Juniperus procera* or *Podocarpus falcatus* came from the central part of the stem or trunk (heartwood) or from the periphery (sapwood).

The number of fragments analysed is too small to enable paleoenvironmental and/or paleoclimatic reconstruction. In addition, they provided only limited insight into the question of the "old-wood" effect (Stouvenot *et al.*, 2013). The matter of chronological inversions is addressed in detail in the presentation of each stratigraphy (see above).

4.4 Synthesis of the radiocarbon ages obtained

The radiocarbon dates span a period of roughly 8000 years. However, three chronological gaps appear in the series, the first around 5000 cal. BP, then from about 4000 to about 2000 cal. BP, and finally the last 400 years (Fig. 16). These gaps in the chronological record correspond either to an interruption of sedimentation (incision) or to the absence of datable material in the sedimentary fill, like at the Mengangebit site.

The synthesis revealed a clear difference in the sedimentation rates between the May Weini site and the other study sites. At the May Weini site, sediment filling took more than two millennia. The sedimentary sequences at the other sites are

[1] https://www.iucnredlist.org/species/42438/2980290#conservation-actions.

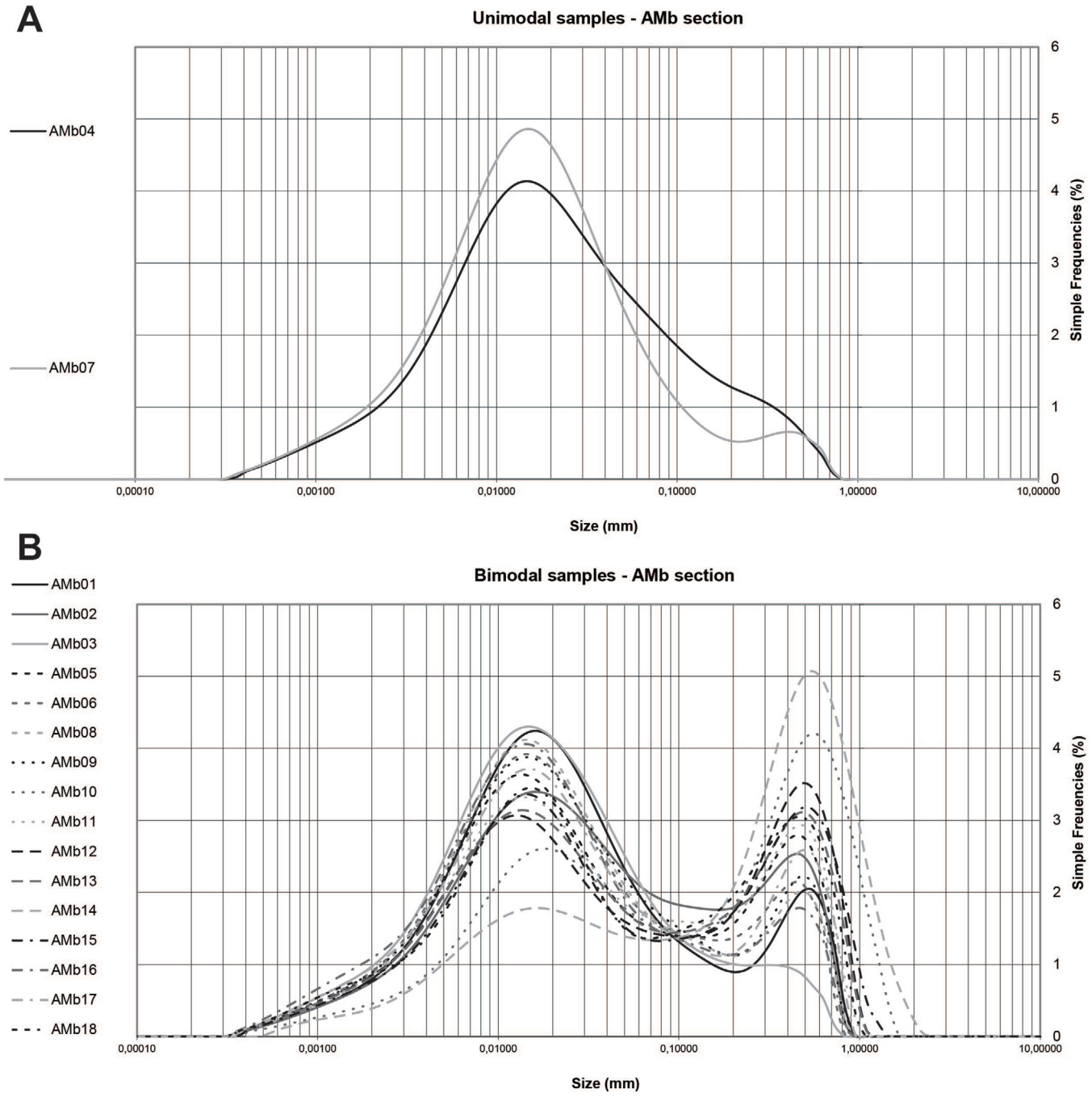

Fig. 19. Grain size curves, AMb section. A: Unimodal samples; B: Bimodal samples.
Fig. 19. *Courbes granulométriques, coupe AMb. A : échantillons unimodaux ; B : échantillons bimodaux.*

marked by a discontinuity between a lower part and an upper part, in which sediments were deposited over a short period of time (the Mengangebit and Ambare Valley sites, in particular). Available data do not allow the building and comparison of age models and to compare them but suggest that the conditions of alluviation in the valley bottoms changed around 6000 cal. BP from slow but continuous sedimentation to alternating aggradation and incision phases.

In the stratigraphic presentation, we mentioned that these phases of rapid aggradation were followed by an incision into the sedimentary fills which sometimes led to the formation of detrital or fluvial terraces. However, it was impossible to identify sites with nested terraces, and we were also unable to estimate the incision rate of the channel over time or to determine when the incision ended. This was particularly the case in the Ambare valley where no ancient sedimentary

records were found, suggesting that older deposits were extensively removed by incision and by the lateral migration of riverbed, but it was not possible to determine the duration of this phase. In the case of Mengangebit, the channel formed in the oldest deposits is filled with sediments which, for the moment, remain impossible to date. At the May Ayni site, the oldest sequence was buried beginning around 2000 years ago, *i.e.*, after a chronological gap lasting almost four millennia during which no stratigraphic information was preserved.

However, we noted a certain synchronism in the phases we were able to identify: an incision around 5900–5500 years ago (May Weini and May Ayni), a resumption of sedimentation around 2000 years ago and an incision affecting the whole watershed, over the last 400 years (Blond *et al.*, 2018; Blond, 2019). Currently, channel entrenchment in alluvial floors is partly masked by terrace cultivation which started to expand in the last quarter of the 20th century (Blond *et al.*, 2018; Blond, 2019). Consequently, although the absence of dates does not allow us to precisely stake out the formation of the sedimentary sequence of May Ayni, we hypothesise that the recent incision also occurred there, like in other reaches of the hydrographic network.

This chronological synthesis also underlines the fact that other morphogenic dynamics were not recorded in the main thalwegs, whereas they seem to have been active at the headwater sites such as Mengangebit. It is impossible to affirm that no aggradation occurred in the main thalwegs between approximately 5000 and 2000 cal. BP, but if aggradation did happen, no trace remains. At least, it should be noted that in the deepest valley, May Weini, the incision was not followed by sufficient aggradation to bury the oldest deposits that form the current alluvial terrace. This suggests that, in this environment, the supply of sediments and the conditions of their transport and deposition have undergone profound changes since around 6000 cal. BP.

All these elements allow us to identify the factors responsible for this geomorphological history and to discuss them in the light of current knowledge of East African environments.

5 Discussion

The results allowed identification of chronological and chronostratigraphic phases. The phases can be linked to sedimentary processes, especially erosive ones. It is possible to identify the drivers of these processes, whether they are biophysical or anthropogenic in origin.

At the scale of the watershed studied here, sediment data point to a role of the location of the section in explaining differences in the chronostratigraphic records. The main differences appear between upstream, intermediate, and downstream parts of the system: some of the oldest deposits (like MWb) are located farthest upstream, while the most recent ones (AMb, in particular) are located downstream; tributaries, which are smaller in size and drain a smaller watershed, have different behaviours (MGb); intermediate sections (MAa) have the advantage of recording processes over a long time span.

These four sections represent a wide chronological range, but this also means that, in most of the samples, it is impossible to compare two different sections in the same period. Nevertheless, this organisation allows a well-documented study of environmental changes over the long period of the Holocene and the identification of their main drivers.

5.1 Holocene climatic changes and their effects on slopes and river systems over the last 8000 years

The Holocene is marked by a wetter period throughout Africa, known as the African Humid Period (AHP) (Le Turdu *et al.*, 1999; Bard *et al.*, 2000; Nyssen *et al.*, 2004; Gascon, 2006; Bubenzer and Riemer, 2007; Armitage *et al.*, 2015; Shanahan *et al.*, 2015), which extended roughly between 12 500 and 5000 BP (Gillespie *et al.*, 1983).

During the Northgrippian stage (Early Holocene), catchments in the study area were marked by low energy sedimentary processes and low aggradation rates. The oldest dated deposits were formed in the May Weini Valley from 8035–7945 cal. BP onward; here, colluviation and alluviation deposited at least 250 cm of silty sediments in almost 2000 years. The colour of sediments and the organic matter content, higher at the base than in the top part of the section, indicate pedogenesis processes, leading to the formation of paleosols, at least up to 5930–5751 cal. BP. In the same area, another previously studied site (Damhalle, see Fig. 4) (Blond *et al.*, 2018), also presents thick silty deposits prior to 7244–6994 cal. BP that have been interpreted as evidence that the morphogenic conditions during the AHP were dominated by colluviation.

Also during the Northgrippian, in our study area, the higher organic matter contents of the sediments can be linked to the growth of vegetation in the valley, favoured by more regular and abundant rainfall. Another possible explanation is that these sediments derive from soils that developed on the slopes covered by vegetation that were subsequently transported over the short distances to the valley bottom by runoff, which would be consistent with the sedimentary characteristics described above. Considering that under current climatic conditions, some big trees including *Ficus sycomorus*, *Juniperus procera* and *Podocarpus falcatus* are still present in this area amongst the otherwise scrubby vegetation, we hypothesise that relatively dense vegetation (forest or shrubs) largely covered the surroundings of Wakarida during the African Humid Period. The absence of coarse sediment and the presence of well-shaped channels suggests that in the rainy season, sheet flows ran through the valley bottoms, without deeply incising the sedimentary infill.

The timing and rhythm of the end of the African Humid Period as well as the transition to drier conditions are widely discussed in the literature. Based on Nile sediments, Butzer (1981) envisages a wet episode in the Ethiopian highlands between 11 200 and 6000 BP, followed by an incision of nearly 15 m, marking an arid phase. Le Turdu *et al.* (1999) envisage a series of wet episodes around the Ziway/Shala Basin between 9500 and 7500 BP, 7000 and 6000 BP and 5850 and 5200 BP. Depending on the authors, the change to arid conditions occurred around 6500–3500 BP (Lüning and Vahrenholt, 2019), around 5800 BP in Egypt (Bubenzer and Riemer, 2007), around 5500 BP at the scale of Africa (Gasse, 2000; Tierney and deMenocal, 2013), at 5160 ± 80 BP at Mai

Makden (Berakhi *et al.*, 1998) or from 4000 BP onwards according to Bonnefille and Umer (1994).

Besides, while Shanahan *et al.* (2015) consider the end of the African Humid Period to be abrupt, *i.e.*, changes occurred over a period of around one century, Moeyersons *et al.* (2006) consider climatic conditions in the Ethiopian highlands deteriorated from 5000 BP onwards, and Dramis *et al.* (2003) indicate a shift towards a more arid climate around 5000–4000 BP, a time-transgressive environmental change.

These differences are partly explained by the fact that the end of the AHP occured later in East Africa than in West Africa (Lézine *et al.*, 2011) and also because in East Africa, climatic controls are more complex to disentangle due to the proximity of the Indian Ocean (Shanahan *et al.*, 2015). In the MWb and MAa sections, the period around and just after 6000 cal. BP marks a transition characterised by the alternation of low-energy and high-energy episodes related to rainfall variability. Locally, one or the other of the trends may take over. Prior to this period, the May Ayni valley records high energy events (Fig. 14). However, only low energy episodes affected May Weini Valley at that time (Fig. 11). This alternation of high and low energy events, not only in the same study area but at the same site, is evidence for the end of the AHP and the transition to a drier climate. The difference in flow energy between sites is also consistent with the fact that local site can control the onset of change: the topographic configuration is very different at the two sites and could at least partly explain the lack of connexion between the deposition processes.

The interruption of sedimentation after 5930–5751 cal. BP at the May Weini site can be related to the analyses of Butzer (1980), who considers the incision of the Nile course and the transition to more arid conditions took place during this period. In the headwater catchments studied here, the factors that triggered this change are not yet entirely clear. On the one hand, with the decrease in the rainfall amount, the supply of sediments may have weakened, involving from then on, the beginning of the progressive incision of a channel into previous deposits. On the other hand, the decrease in rainfall amount may have been offset by an increase in rainfall intensity, which is a quite common characteristic of dry climates. In this case, higher discharges, even if they are rare, favour sediment erosion. The observed time gap between the downstream and upstream parts of the catchment could thus be explained by the time required to transfer the sediments to the stream bed. Despite this uncertainty, available observations suggest a shift towards drier conditions and aridification around and after 6000 cal. BP, which is consistent with the hiatus in the sedimentation at May Ayni, where no sediments date to between 5715–5590 cal. BP and 1870–1720 cal. BP. This may be linked with the erosional phase identified by Berger *et al.* (2012), starting from 5200 BP in the Hadramawt watershed (Yemen).

At the scale of the watershed studied here, this hiatus is only interrupted by the succession of detrital units on the Mengangebit cone. The absence of alluvial deposits in the main valleys suggests that sedimentary supply mostly affected headwater parts and not the fluvial continuum, perhaps due to weakening of the transport capacity over long distances. This suggests a period of instable climatic conditions, during which the drying could have occurred approximately 6000 years ago up to 2000 years ago, in line with the conclusions drawn by other authors who point to a progressive end of the African Humid Period (see for example Hély *et al.*, 2009; Liu *et al.*, 2017), during which dry phases alternate with humid ones: around Adwa, Machado *et al.* (1998) observed three main humid phases from 4000 to 690 BP, while Gebru *et al.* (2009) identified an arid phase from 5500 to 2550 cal. BP, interspersed with three humid phases.

The two last millennia appear to be marked by notable climatic and environmental variations at the local scale. For example, D'Andrea *et al.* (2008) indicate a wet phase on the Tigray plateau from 500 BC onwards and a period of more abundant seasonal rainfall in the Adwa and Aksum region between 100 BC and 400 BC, which is also echoed by Fattovich (2010), who describes a minor wet phase from 500 BC to 500 AD, while Nash *et al.* (2016) describe a pronounced arid phase between 200 BC and 200 AD, followed by slightly wetter conditions between 200 and 600 AD, and episodes of heavier rainfall between 700 and 1000 AD. But the documented presence of populations in the area makes the climatic changes more difficult to disentangle from anthropogenic factors.

5.2 Socio-ecological systems and impacts of anthropization

The Tigray plateau has been inhabited since the end of the Pleistocene (Finneran, 2007) and during the prehistoric period (French *et al.*, 2009), and was cultivated during those periods (Graziosi, 1941). However, the pre- and proto-Aksumite period (800–50 BC, see D'Andrea *et al.*, 2008; Fattovich, 2010; Pietsch and Machado, 2014), and the Aksumite period (50 BC–700 AD, D'Andrea *et al.*, 2008; Fattovich, 2010) are generally considered to have seen significant demographic and agricultural development (D'Andrea *et al.*, 2008; Phillipson, 2009; Fattovich, 2010; Benoist *et al.*, 2020; Benoist *et al.*, 2021). If the pre-Aksumite, proto-Aksumite and Aksumite human occupations are well known in different sites of the Tigray (Anfray, 1990; Bard *et al.*, 2000; Bard *et al.*, 2014), the previous period is less well known (Finneran, 2007) and possible human control of their environment may be recorded in sedimentary archives.

In the Mengangebit deposits studied here, the alternation of thin material and coarser beds points to a shift from low energy to higher energy flows. As mentioned above, this shift may be linked to direct effects (rainfall intensity) or indirect effects (density of the vegetation cover) of changes linked to climatic conditions. Nevertheless, changes in the vegetation cover could have been caused by clearing or burning some of the surrounding slopes. Indeed, according to several authors, it cannot be excluded that human groups populated the Tigray at that time and that occupation may have caused the first deforestation (Berakhi *et al.*, 1998; Bard *et al.*, 2000; Darbyshire *et al.*, 2003; Gebru *et al.*, 2009). Opening the vegetation may have made the slopes more sensitive to water erosion, all the more, if these changes were combined with climatic conditions more favourable to concentrated runoff. However, as no archaeological remains of this age were found on the site or in the vicinity, it is not possible to verify this hypothesis.

If geoarchaeological studies at other Tigray sites have produced evidence of agriculture in the form of both plant and animal remains from the first half of the 1st millennium BC (Bard *et al.*, 2000; Phillipson and Phillips, 2000; D'Andrea *et al.*, 2008), in our study area, a long gap (almost two millennia) appears, between roughly 4000 and 2000 years ago (Fig. 16). It is thus difficult to document the impact of the beginning of the Aksumite period using chronostratigraphic results. Such a gap can also be found at other sites, like Damhalle (Fig. 4), where the section presents a hiatus between 7244–6994 cal. BP and 4150–3977 cal. BP (Blond *et al.*, 2018). In both cases, this gap could be explained by erosion of the sediments deposited during this period by later high energy events. As demonstrated in the previous section, this may be linked to a shift toward drier conditions. Higher energy events may also be the result of a stronger impact of the societies on their environments. Indeed, people living in the region cut wood for heating and construction and probably cleared vegetation on the slopes for the purpose of cultivation. In the early days, their homes may have taken the form of light wooden constructions (tukul), as these still exist today, and which require the felling of many trees for their construction (Nyssen *et al.*, 2010).

Clearing led to the removal of the soil that had formed under the vegetation cover on the slopes. The soil was then deposited in the valley bottoms. Evidence for the Aksumite period is quite tenuous – although it cannot be excluded that some deposits from this period were not preserved – since only four charcoals originating from that time could be dated at two sites (1816–1618 cal. BP and 1530–1386 cal. BP at AMb and 1870–1720 cal. BP and 1822–1626 cal. BP at MAa). Observations indicate that some valleys still had quite fine and continuous deposits during this period. This suggests that, during this period, at least in the MAa and AMb sectors, catchments were marked by low energy processes and by storage of fine-grained sediment on the valley floors. This can be explained on the one hand by climatic conditions, which Butzer (1981) says are more humid in the 1st century AD and led to an improvement in agriculture (see above) as well as by biostasic conditions on slopes. In the Ambare Valley, the deposition of undisturbed fine sediments for more than a millennium before 625–506 cal. BP suggests there was no agricultural use of the valley floor (but does not invalidate the hypothesis of the opening of clearings or slash-and-burn agriculture on the slopes). The shape of the valley, which is very narrow and partly downstream of the local watershed, combined with the higher precipitation reported by Butzer (1981) suggests that this valley bottom was marshy – at least seasonally – during the Aksumite period. Another possible explanation is the distance of the area from the urban centre of Wakarida (more than 3 km as the crow flies, through rather steep valleys). As the area of Ambare is located far from this urban centre, it may not have been used for agriculture. Nevertheless, during this period, the processes are generally low energy, and if human activity had caused an erosion crisis in local environments, it would certainly be perceptible in stratigraphic records in so far as the Ambare valley includes a more than 33-km^2 catchment and its narrowness and longitudinal profile allow high energy flows and the movement of coarse grained sediments. Thus, we cannot exclude the possibility that erosion processes could have been controlled by Aksumite societies. The period of the end of the Aksumite kingdom does not clearly appear in sedimentary records around Wakarida, except for one date (1289–1150 cal. BP), which corresponds to the decline of human presence in Aksum. However, it is difficult to support the hypothesis developed by Butzer (1981) that soil degradation and environmental conditions coincide with the fall of the kingdom: at the site of Ambare, the charcoal is part of an accumulation that continued until 625–506 cal. BP, a period which conversely appears to be a time of major morphogenic changes in the study area.

The post-Aksumite period begins around 700 AD (D'Andrea *et al.*, 2008) and is less well documented, especially between the 9th and 12th centuries AD, sometimes called the "Dark Ages" (Finneran, 2007). Around the 8th century AD, Aksumite power was declining due to political and economic competition. The kingdom was invaded by Bedja populations during the 7th and 8th centuries AD (El Fāsī and Hrbek, 1990), Aksum was cut off from its commercial relations with the Byzantine and Persian empires and the Arabs destroyed the Aksumite fleet and the port of Adulis at the beginning of the 8th century (Finneran, 2007). In the 9th century AD, the capital of the declining kingdom moved southwards towards Lake Hayk and, according to tradition, Queen Yudit completed its disappearance with her conquest in 980 (Butzer, 1981). The population became scarcer and power progressively shifted towards the south (Bard *et al.*, 2000; Gascon, 2006; Derat *et al.*, 2021).

In our survey area, the 10th–12th centuries were marked by the reoccupation of the ruins of Wakarida with lightweight homes (tents or huts?) and probably intermittent human presence (Gajda *et al.*, 2017). This light occupation is consistent with the absence of evidence of anthropogenic disturbance (development of a paleosol in Ambare valley), but could also be related to the location of the AMb accumulation at the very end of the local watershed, in a space that is not easily accessible and is far from the main centre of Wakarida.

The end of the Middle Ages was marked by the appearance of the Zagwe dynasty in Lasta, around Lalibella in the 13th century AD (Finneran, 2007; Fauvelle *et al.*, 2010; Bosc-Tiessé *et al.*, 2014). This shift in the economic and political heart of the Ethiopian kingdom may at least partially explain the small number of sedimentary records in the region for this period: the transfer of the capital from the north to the south may have caused a population decline resulting in reconquest by vegetation and a return to biostasic conditions.

In our study area, the modern period is documented less by the number of charcoal samples dated from that time than by the information that can be derived from chronological inversions. The accumulations in the Ambare Valley are indeed marked by two inversion phases, which correspond to ages between 1816–1618 cal. BP and 625–506 cal. BP on the one hand, and between 1530–1386 cal. BP and 530–335 cal. BP on the other hand. These two phases indicate a *terminus ante quem* approximately between 600 and 300 cal. BP (Fig. 17), representing the main period of development of a braided channel. The mixture of dates indicates that the charcoals originated from different primitive sources and were reworked over time. The soils that had developed under the

plant cover on the slopes in previous periods (from 1816–1618 cal. BP to 530–335 cal. BP), were eroded and deposited in the valleys, probably after relatively brief alluvial movements.

The erosion of slope deposits is evidence for opening of vegetation on slopes, probably for domestic uses (as firewood or construction material) and/or for agriculture. Such a disturbance can be found in Aksum between the abandonment of the site around the 7th century and the 15th–17th centuries AD. Butzer (1981) detected no destabilization of the system, which only occurred in the 15th–17th centuries. However, the effects of climate change in destabilising the slopes cannot be overlooked. In the study area, the deposits in the period identified as *terminus ante quem* contain many coarse elements, compatible with an increase in competent flows indicating increased rainfall, as can be found elsewhere in Africa between 1400 and 1700 AD (Darbyshire *et al.*, 2003). Anthropogenic control factors are observed, but they may also have been catalysed by wet phases.

These elements underline the importance of dates that, at first glance, may appear to be errors and therefore be rejected. Here, chronological consistency is not respected: older ages follow more recent ones, which is to the reverse of the usual order of sedimentary filling. These chronological inversions could be errors in dating, pollution or contamination, or even sampling errors or uncertainty concerning the deposit sources of the charcoal collected (Delibrias and Giot, 1970; Evin, 1977). These dates could then have simply been rejected. However, we considered it important to consider them first in relation to the other dates of the accumulation to which they belong, and secondly to also interpret them with respect to the stratigraphy in which the charcoals were collected. Thus, chronological inversions can indicate soil changes and therefore be a valuable indicator in elucidating different processes: anthropization of a space, crossing a threshold linked to anthropogenic actions or climate or vegetation changes. They can provide time limits for dynamic equilibrium disruption or threshold crossings within sedimentary cascades (Cossart, 2016).

6 Conclusion

This chronostratigraphic study made it possible to identify several phases in the establishment of the current landscapes around the Wakarida site, partly by paying particular attention to the chronological inversions and their heuristic in understanding sedimentary cascades. First, during the Northgrippian (Early Holocene), sediments indicate that the valleys were gradually filled by low energy colluvial and/or alluvial processes, which allowed the accumulation of a significant thickness of sediments that, in some cases, evolved through hydromorphism. During the early Meghalayan (Middle Holocene) ablation processes were established, attesting on the one hand to the increasing irregularity of precipitation, but also to the destabilisation of the vegetation cover on the slopes. The destabilisation may be the result of human actions in the region, even if such actions are not corroborated by archaeological evidence. Finally, in the last 2000 years, the impact of populations on their environment, in connection with the development (then decline) of the Aksumite kingdom, was felt, particularly through the opening up of the vegetation on the slopes. However, it is particularly around the 14th–17th centuries AD that the effects of anthropization on morphogenic processes seem to be the most important. It is possible that a threshold was crossed at this time, due to the depletion of available sedimentary stocks on the slopes. Even though human activities probably modified the environment for more than a millennium, this threshold would have disturbed the sedimentary cascades. In the last 400 years, nothing more has been recorded in the sediments.

Acknowledgements. The authors would like to thank the reviewers and editors for comments and suggestions. We also thank the archaeological and epigraphic mission of Wakarida and its directors for their collaboration, as well as the Archéorient laboratory (UMR 5133) for the resources made available, the CFEE (French Centre for Ethiopian Studies) for logistical support in Ethiopia, the OMEAA platform in Lyon for the analyses, and the Université Lumière Lyon 2. This study would not have been possible without the financial and material support of the universities and laboratories that the multi-year research programming law threatens to weaken and destabilize by increasing the logic of competition and the precariousness of our research activities.

References

Anfray F. 1990. Les anciens Éthiopiens : siècles d'histoire. A. Colin.

Armitage SJ, Bristow CS, Drake NA. 2015. West African monsoon dynamics inferred from abrupt fluctuations of Lake Mega-Chad. *Proceedings of the National Academy of Sciences* 112(28): 8543–8548.

Bard KA, Coltorti M, DiBlasi MC, *et al.* 2000. The environmental history of Tigray (Northern Ethiopia) in the Middle and Late Holocene: A preliminary outline. *Afr. Archaeol. Rev.* 17(2): 65–86.

Bard KA, Fattovich R, Manzo A, *et al.* 2014. The chronology of Aksum (Tigrai, Ethiopia): A view from Bieta Giyorgis. *Azania: Archaeological Research in Africa* 49(3): 285–316.

Bascom J, ed. 2015. *National Atlas of Ethiopia*. Addis-Abeba: Ethiopian Mapping Agency.

Bekele-Tesemma A, Tengnäs B. 2007. Useful trees and shrubs of Ethiopia: Identification, propagation, and management for 17 agroclimatic zones. Technical Manual No. 6. Nairobi: RELMA in ICRAF Project, World Agroforestry Centre, Eastern Africa Region.

Benoist A, Gajda I, Matthews S, *et al.* 2020. On the nature of South Arabian influences in Ethiopia during the late first millennium BC: Late pre-Aksumite settlement on the margins of the eastern Tigray plateau. In: *Proceedings of the Seminar for Arabian Studies: Papers from the Fifty-Third Meeting of the Seminar for Arabian Studies held at the University of Leiden from Thursday 11th to Saturday 13th July 2019*, 50: 19–36.

Benoist A, Gajda I, Schiettecatte J, *et al.* 2021. What was the South Arabian impact on the development of Ethiopian margins in Antiquity? Evolution of settlement patterns in the Wakarida Region from pre-Aksumite to Late Aksumite periods. In: Hatke G, Ruzicka R, eds. *South Arabian long-distance trade in Antiquity: "Out of Arabia"*. Cambridge Scholars Publishing, pp. 111–153.

Berakhi O, Brancaccio L, Calderoni G, *et al.* 1998. The Mai Maikden sedimentary sequence: A reference point for the environmental evolution of the Highlands of Northern Ethiopia. *Geomorphology* 23(2-4): 127–138.

Berger J-F, Bravard J-P, Purdue L, *et al.* 2012. Rivers of the Hadramawt watershed (Yemen) during the Holocene: Clues of late functioning. *Quaternary International* 266: 142–161.
Billi P, ed. 2015. Landscapes and landforms of Ethiopia. Dordrecht: Springer Netherlands.
Blond N. 2019. Dynamiques sédimentaires holocènes et terrasses agricoles dans les montagnes du Tigray oriental (Éthiopie). Thèse de doctorat, Université Lumière Lyon 2, France, 626 p.
Blond N, Jacob-Rousseau N, Callot Y. 2018. Terrasses alluviales et terrasses agricoles. Première approche des comblements sédimentaires et de leurs aménagements agricoles depuis 5000 av. n. è. à Wakarida (Éthiopie). *Géomorphologie* 24(3): 277–300.
Blott SJ, Pye K. 2001. GRADISTAT: A grain size distribution and statistics package for the analysis of unconsolidated sediments. *Earth Surf. Proc. Land* 26(11): 1237–1248.
Bonnefille R, Umer M. 1994. Pollen-inferred climatic fluctuations in Ethiopia during the last 3000 years. *Palaeogeogr. Palaeoecol.* 109 (2-4): 331–343.
Bosc-Tiessé C, Derat M-L, Bruxelles L, *et al.* 2014. The Lalibela Rock Hewn Site and its Landscape (Ethiopia): An archaeological analysis. *J. Afr. Archaeol.* 12(2): 141–164.
Bronk Ramsey CB. 2017. Methods for summarizing radiocarbon datasets. *Radiocarbon* 59(6): 1809–1833.
Bubenzer O, Riemer H. 2007. Holocene climatic change and human settlement between the central Sahara and the Nile Valley: Archaeological and geomorphological results. *Geoarchaeology* 22 (6): 607–620.
Butzer KW. 1980 Pleistocene history of the Nile Valley in Egypt and Lower Nubia. In: Williams M, Faure H, eds. *The Sahara and the Nile*, pp. 238–252.
Butzer KW. 1981. Rise and fall of Axum, Ethiopia: A geo-Archaeological interpretation. *Am. Antiq.* 46(3): 471–495.
Carcaillet C, Talon B. 2007. Aspects taphonomiques de la stratigraphie et de la datation de charbons de bois dans les sols : exemple de quelques sols des Alpes. *Geogr. Phys. Quat.* 50(2): 233–244.
Chamley H. 1987. Sédimentologie. Collection « Géosciences ». Paris : Dunod.
Chernet T. 1988. Hydrogeological map of Ethiopia. Addis-Abeba, Ethiopia: Ministry of Mines and Energy, Ethiopian Institute of Geological Surveys.
Cossart E. 2016. L'(in)efficacité géomorphologique des cascades sédimentaires en question : les apports d'une analyse réseau. *Cybergeo: European Journal of Geography.*
Couralet C, Bakamwesiga H. 2007. Juniperus procera Hochst. ex Endl. In: *PROTA (Plant Resources of Tropical Africa/Ressources Végétales de l'Afrique Tropicale)*. Wageningen, Netherlands. Available from https://www.prota4u.org/database/protav8.asp?h=M4&t=Juniperus,procera&p=Juniperus+procera#Synonyms.
Cubizolle H. 2009. Paléoenvironnements. Paris : A. Colin.
D'Andrea AC, Manzo A, Harrower MJ, *et al.* 2008. The pre-Aksumite and Aksumite settlement of NE Tigrai, Ethiopia. *J. Field Archaeol.* 33(2): 151–176.
Darbyshire I, Lamb H, Umer M. 2003. Forest clearance and regrowth in northern Ethiopia during the last 3000 years. *The Holocene* 13 (4): 537–546.
Delibrias G, Giot P-R. 1970. Inadéquation, hétérogénéité et contamination des échantillons soumis pour les datations radiocarbone. *Bull. Soc. Prehist. Fr.* (Comptes rendus des séances mensuelles) 67(5): 135–137.
Derat M-L, Bosc-Tiessé C, Garric A, *et al.* 2021. The rock-cut churches of Lalibela and the cave church of Washa Mika'el: Troglodytism and the Christianisation of the Ethiopian Highlands. *Antiquity* 95(380): 467–486.
Dramis F, Umer M, Calderoni G, *et al.* 2003. Holocene climate phases from buried soils in Tigray (Northern Ethiopia): Comparison with lake level fluctuations in the Main Ethiopian Rift. *Quat. Res.* 60(3): 274–283.
Dugast F, Gajda I. 2010. Report on fieldwork – Preliminary survey in Tigray Region, Ethiopia (March 22nd–April 2nd 2010). French-Ethiopian Project of Archaeological and Epigraphic Investigations in Tigrai region, Ethiopia pre-Aksumite and Aksumite period (8th c. BC–AD 7th c.).
Edwards S, Egziabher TBG, Araya H. 2007. Successes and challenges in ecological agriculture: experiences from Tigray, Ethiopia. In: Ching LL, Edwards S, Scialabba NE-H, eds. *Climate change and food systems resilience in Sub-Sahran Africa*. Rome, Italy: FAO, pp. 231–294.
El Fāsī M, Hrbek I, eds. 1990. Histoire générale de l'Afrique. *Tome 3 : L'Afrique du VII^e^ au XI^e^ siècle*. Paris : Unesco.
El-Juhany L. 2014. Cross section characteristics and age estimation of Juniperus procera trees in the natural forests of Saudi Arabia. *J. Pure Appl. Microbio.* 8: 657–665.
Evin J. 1977. Critères de choix des échantillons pour la datation par le radiocarbone. *Bull. Soc. Prehist. Fr.* 74(5): 135–138.
Farjon A. 2005. A monograph of Cupressaceae and Sciadopitys. Kew: Royal Botanic Gardens, Kew Publishing.
Fattovich R. 2010. The development of ancient states in the Northern Horn of Africa, c. 3000 BC-AD 1000: An archaeological outline. *J. World Prehist.* 23(3): 145–175.
Fauvelle F-X, Bruxelles L, Mensan R, *et al.* 2010. Rock-cut stratigraphy: Sequencing the Lalibela churches. *Antiquity* 84(326): 1135–1150.
Finneran N. 2007. The archaeology of Ethiopia. London, New York: Routledge.
Folk RL, Ward WC. 1957. Brazos River bar [Texas]: A study in the significance of grain size parameters. *J. Sediment. Res.* 27(1): 3–26.
French C, Sulas F, Madella M. 2009. New geoarchaeological investigations of the valley systems in the Aksum area of northern Ethiopia. *CATENA* 78(3): 218–233.
Friedman GM, Sanders JE. 1978. Principles of sedimentology. New York: John Wiley & Sons, Ltd.
Friis I, Sebsebe D, van Breugel P. 2010. Atlas of the potential vegetation of Ethiopia. *Biologiske skrifter* 58. Copenhagen: Det Kongelige Danske Videnskabernes Selskab.
Gajda I, Benoist A, Charbonnier J, *et al.* 2017. Wakarida, un site aksumite à l'est du Tigray : fouilles et prospections 2011–2014. In: *Dossier: Women, Gender and Religions in Ethiopia*. Annales d'Éthiopie Special Issue. Paris : Éditions de Boccard, pp. 175–222.
Gascon A. 2006. Sur les hautes terres comme au ciel : identités et territoires en Éthiopie. Paris : Publications de la Sorbonne.
Gasse F. 2000. Hydrological changes in the African tropics since the Last Glacial Maximum. *Quat. Sci. Rev.* 19(1-5): 189–211.
Gebru T, Eshetu Z, Huang Y, *et al.* 2009. Holocene palaeovegetation of the Tigray Plateau in northern Ethiopia from charcoal and stable organic carbon isotopic analyses of gully sediments. *Palaeogeogr. Palaeocl.* 282(1-4): 67–80.
Gillespie R, Street-Perrott FA, Switsur R. 1983. Post-glacial arid episodes in Ethiopia have implications for climate prediction. *Nature* 306(5944): 680–683.
Gob F, Bravard J-P, Petit F. 2010. The influence of sediment size, relative grain size and channel slope on initiation of sediment motion in Boulder Bed Rivers. A lichenometric study. *Earth Surf. Process.* 35(13): 1535–1547.
Goldberg P, Macphail RI. 2006. Practical and theoretical geo-archaeology. Malden, MA; Oxford: Blackwell Publishing.
Graziosi P. 1941. Le Pitture rupestri dell'Amba Focadà (Eritrea). *Rassegna Di Studi Etiopici* 1(1): 61–70.

Heiri O, Lotter AF, Lemcke G. 2001. Loss on ignition as a method for estimating organic and carbonate content in sediments: Reproducibility and comparability of results. *J. Paleolimnol.* 25(1): 101–110.

Hély C, Braconnot P, Watrin J, *et al.* 2009. Climate and vegetation: Simulating the African humid period. *C. R. Geosci.* 341(8-9): 671–688.

Inman DL. 1952. Measures for describing the size distribution of sediments. *SEPM Journal of Sedimentary Research* 22.

Kazmin V. 1976. Geological Map of Ethiopia – Adigrat (ND 37-7). 1:25 000. Addis-Ababa: Geological Survey of Ethiopia, Ministry of Mines, Energy and Water Resources.

Le Turdu C, Tiercelin J-J, Gibert E, *et al.* 1999. The Ziway-Shala Lake Basin system. Main Ethiopian Rift: Influence of volcanism, tectonics, and climatic forcing on basin formation and sedimentation. *Palaeogeogr. Palaeocl.* 150(3-4): 135–177.

Lézine A-M, Hély C, Grenier C, *et al.* 2011. Sahara and Sahel vulnerability to climate changes, lessons from Holocene hydrological data. *Quat. Sci. Rev.* 30(21): 3001–3012.

Liu X, Rendle-Bühring R, Kuhlmann H, *et al.* 2017. Two phases of the Holocene East African humid period: Inferred from a high-resolution geochemical record off Tanzania. *Earth Planet. Sci. Lett*.

Lüning S, Vahrenholt F. 2019. Holocene climate development of North Africa and the Arabian Peninsula. In: Bendaoud A, Hamimi Z, Hamoudi M, *et al.*, eds. *The Geology of the Arab World – An overview*. Springer International Publishing, pp. 507–546.

Machado MJ, Pérez-González A, Benito G. 1998. Paleoenvironmental changes during the last 4000 years in the Tigray, Northern Ethiopia. *Quat. Res.* 49(03): 312–321.

Maydell HJ von. 1990. Trees and Shrubs of the Sahel: Their characteristics and uses. Weikersheim: Josef Margraf.

Moeyersons J, Nyssen J, Poesen J, *et al.* 2006. Age and backfill/overfill stratigraphy of two tufa dams, Tigray Highlands, Ethiopia: Evidence for Late Pleistocene and Holocene wet conditions. *Palaeogeogr. Palaeoecol.* 230(1-2): 165–181.

Nash DJ, De Cort G, Chase BM, *et al.* 2016. African hydroclimatic variability during the last 2000 years. *Quat. Sci. Rev.* 154: 1–22.

Neumann K, Schoch W, Détienne P, *et al.* 2001. Woods of the Sahara and the Sahel. An anatomical atlas. Bern: Paul Haupt.

Nyssen J, Poesen J, Moeyersons J, *et al.* 2004. Human impact on the environment in the Ethiopian and Eritrean Highlands – A state of the art. *Earth-Sci. Rev.* 64(3): 273–320.

Nyssen J, Frankl A, Munro RN, *et al.* 2010. Digital photographic archives for environmental and historical studies: An example from Ethiopia. *Scott. Geogr. J.* 126(3): 185–207.

Pelling R, Campbell G, Carruthers W, *et al.* 2015. Exploring contamination (intrusion and residuality) in the archaeobotanical record: Case studies from central and southern England. *Veg. Hist. Archaeobot.* 24(1): 85–99.

Phillipson DW. 2009. The first millennium BC in the highlands of Northern Ethiopia and South-Central Eritrea: A reassessment of cultural and political development. *Afr. Archaeol. Rev.* 26(4): 257–274.

Phillipson DW, Phillips JS. 2000. Archaeology at Aksum, Ethiopia, 1993–1997. British Institute in Eastern Africa: Society of Antiquaries of London.

Pietsch D, Machado MJ. 2014. Colluvial deposits-proxies for climate change and cultural chronology. A case study from Tigray, Ethiopia. *Z. Geomorphol. Supp.* 58(1): 119–136.

Reimer PJ, Bard E, Bayliss A, *et al.* 2013. IntCal13 and Marine13 radiocarbon age calibration curves 0–50 000 years cal. BP. *Radiocarbon* 55(4): 1869–1887.

Ruffo CK, Birnie A, Tengnäs B. 2002. Edible wild plants of Tanzania. Nairobi, Kenya: Regional Land Management Unit/Sida.

Schweingruber FH. 1990. Anatomy of European Wood: An atlas for the identification of European trees, shrubs and dwarf shrubs. Bern, Stuttgart: Paul Haupt.

Shanahan TM, McKay NP, Hughen KA, *et al.* 2015. The time-transgressive termination of the African humid period. *Nat. Geosci.* 8(2): 140–144.

Stouvenot C, Beauchêne J, Bonnissent D, *et al.* 2013. Datations radiocarbone et le « problème vieux bois » dans l'arc antillais : état de la question. In: *25to Congreso Internacional de Arqueología del Caribe – 25th International Congress for Caribbean Archeology – 25e Congrès International de l'Archéologie de la Caraïbe*, San-Juan (Puerto Rico), Instituto de Cultura Puertorriqueña, el Centro de Estudios Avanzados de Puerto Rico y el Caribe y la Universidad de Puerto Rico, Recinto de Río Piedras, pp. 459–494.

Tierney JE, deMenocal PB. 2013. Abrupt shifts in horn of Africa hydroclimate since the last glacial maximum. *Science* 342(6160): 843–846.

Trask PD. 1930. Mechanical analyses of sediments by centrifuge. *Econ. Geol.* 25(6): 581–599.

Cite this article as: Blond N, Jacob-Rousseau N, Bouchaud C, Callot Y. 2021. From section to landscape(s): reconstructions of environmental and landscape changes for the past 8000 years around the site of Wakarida (Ethiopia) using chronostratigraphy, *BSGF - Earth Sciences Bulletin* 192: 53.